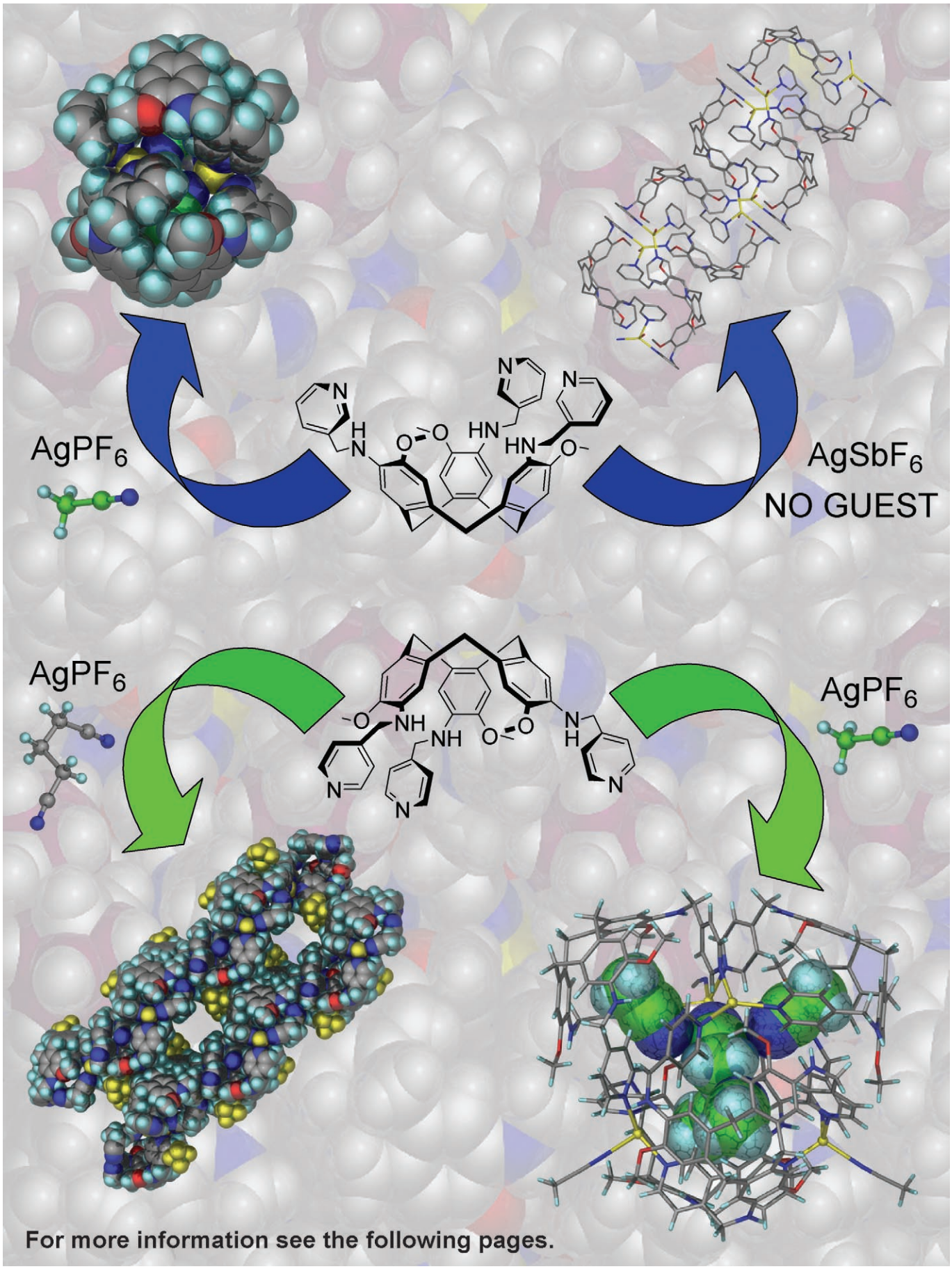

CHEMISTRY
A EUROPEAN JOURNAL

DOI: 10.1002/chem.200501542

Tris(pyridylmethylamino)cyclotriguaiacylene Cavitands: An Investigation of the Solution and Solid-State Behaviour of Metallo-Supramolecular Cages and Cavitand-Based Coordination Polymers

Christopher J. Sumby,[a] Julie Fisher,[a] Timothy J. Prior,[b] and Michaele J. Hardie*[a]

Abstract: The synthesis of the three isomeric tris(pyridylmethylamino)cyclotriguaiacylene cavitands is reported, along with the crystal structures of the 2- and 4-pyridyl derivatives. The generality of a previously described $[Ag_2\{tris(3\text{-pyridylmethylamino})cyclotriguaiacylene\}_2]^{2+}$ dimeric capsule motif and the $[Ag_4\{tris(4\text{-pyridylmethylamino})cyclotriguaiacylene\}_4]^{4+}$ tetrahedron with several silver salts was confirmed in the solid state and the corresponding solution species were investigated by NMR spectroscopy. Host–guest interactions in these systems have been probed and these interactions are demonstrated to alter and influence the self-assembly outcome of the reaction. Notably, introduction of larger glutaronitrile guest molecules to the $[Ag_4L_4]^{4+}$ tetrahedron system prevents formation of the tetrahedral structure, resulting instead in the formation of a 4.8^2 coordination network in the solid state. In the absence of templating acetonitrile guests in the $[Ag_2(\mathbf{3})_2]^{2+}$ capsule system, formation of a cage-based one-dimensional coordination polymer is observed.

Keywords: coordination polymers · host–guest systems · ligand design · silver · supramolecular chemistry

Introduction

The trigonal pyramidal cavitand cyclotriveratrylene (CTV) has previously found application as a molecular host,[1,2] a precursor to cryptophanes and hemicryptophanes,[3] and a component in hydrogen-bonded or coordination networks.[4,5] The shallow cavity imparted by the crown conformation of CTV also makes it an ideal core to prepare functionalised derivatives for the construction of discrete metallo-supramolecular assemblies and infinite coordination networks. In both these goals, the CTV framework can offer a number of advantages over planar cores favoured in the literature. For discrete assemblies, a bowl-shaped cavitand functionalised with appropriate donor groups can present a convergent binding mode and can potentially form assemblies with greater internal volumes than a corresponding planar analogue. For coordination networks, trigonal pyramidal cavitands provide a number of advantages; namely,

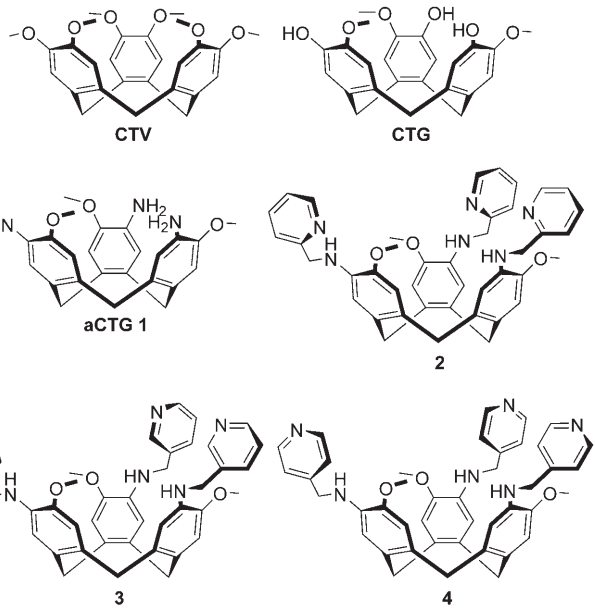

[a] Dr. C. J. Sumby, Dr. J. Fisher, Dr. M. J. Hardie
School of Chemistry, University of Leeds
Leeds LS2 9JT (UK)
Fax: (+44) 113-343-6565
E-mail: m.j.hardie@leeds.ac.uk.

[b] Dr. T. J. Prior
CCLRC Daresbury Laboratory, Daresbury
Warrington, WA4 4AD (UK)

Supporting information for this article is available on the WWW under http://www.chemeurj.org/ or from the author. Supporting Information for this article includes tables of diffusion coefficients and crystal data for additional structures.

unusual ligand geometries, multiple inclusion behaviours and the possibility of using host–guest synthons to control the assemblies.

CTV, through its demethylated derivative cyclotricatechylene, and its trihydroxy analogue cyclotriguaiacylene (CTG) have previously been utilised as starting materials for the synthesis of ligands for transition metals. A handful of ligands have been prepared with these precursors incorporating thiols[6] catechols,[7] and *N*-heterocyclic donor functionalities.[8,9] We have reported a number of new compounds with *N*-heterocyclic donor groups including pyridine, quinoline, quinoxaline and terpyridine,[10] of which some have shown considerable promise as building blocks for coordination polymers.[11] These coordination polymers display a number of interesting properties such as multiple inclusion behaviour and templation by host–guest interactions.

The controlled assembly of various molecular architectures, such as two-dimensional polygons and three-dimensional polyhedra, from linear and angular components has progressed significantly over the last decade.[12] This encompasses the synthesis of comparatively small M_3L_2 assemblies[13] to considerably larger polyhedra formed from 36 components.[14] While a significant number of examples of metallo-supramolecular polyhedra have been reported with planar ligand components, relatively scant attention has been directed toward the formation of such species from cavitands. Additionally, many of the examples of polyhedra incorporating cavitands are formed from fourfold symmetric cavitands.[15] Larger cavitand-based metallo-supramolecular structures with more than two cavitands are rare, but include a tetrahedral structure, in which calixresorcinarene ligands act as the vertices of a metallo-supramolecular tetrahedron,[16,17] and hexameric spheroidal capsules with the formula $Ga_{12}L_6$,[18] closely related to the corresponding hydrogen-bonded hexameric assemblies.[19]

More recently we have reported the use of tris(pyridylmethylamino)cyclotriguaiacylene cavitands for the formation of $[Ag_2(\mathbf{3})_2(CH_3CN)_2]^{2+}$ dimeric capsules and $[Ag_4(\mathbf{4})_4(CH_3CN)_4]\cap\cdot 4\,CH_3CN$ tetrahedral metallo-supramolecular prisms with a spiked pyramidal aspect from $AgPF_6$ and $AgBF_4$, respectively.[20] The ligands employed in the formation of these cage species were constructed upon a CTV skeleton that has been derivatised with amine functional groups (aCTG, **1**). Herein we report full details of the preparation of the three amine ligands, and the solid-state structures of **2** and **4**. The generality of the $[Ag_2(\mathbf{3})_2]^{2+}$ dimeric capsule motif and the $[Ag_4(\mathbf{4})_4]^{4+}$ tetrahedron with AgX (in which $X = BF_4^-$, PF_6^-, SbF_6^-, $(OSO_2CF_3)^-$, $[Co(C_2B_9H_{11})_2]^-$, $(CB_{11}H_{12})^-$) in the solid state are reported, and the species formed in solution were studied by a variety of NMR techniques and mass spectrometry. Not only have we investigated the capsule- and cage-forming abilities of these cavitands, but we have also been able to alter and influence the self-assembly outcome by host–guest interactions. Introduction of a larger glutaronitrile guest molecule to the $[Ag_4L_4]^{4+}$ tetrahedron system perturbs the tetrahedral structure leading to the formation of a 4.8^2 coordination network in the solid state, while the absence of acetonitrile in the $[Ag_2(\mathbf{3})_2]^{2+}$ capsule system results in a one-dimensional coordination polymer. These two new coordination polymers, formed with $AgPF_6$ and $Ag[Co(C_2B_9H_{11})_2]$, or $AgSbF_6$, respectively, were characterised by X-ray crystallography and their structures, and the relationship to their related cage compounds, discussed herein.

Results and Discussion

Ligand synthesis and solid-state behaviour: The entrance point into the amine-linked CTV ligands was through (±)-3,8,13-triamino-2,7,12-trimethoxy-10,15-dihydro-5*H*-tribenzo[*a*,*d*,*g*]cyclononene (aCTG, **1**), which can be prepared by a literature procedure starting from commercially available 4-nitro-3-methoxybenzyl alcohol. This common intermediate can readily be synthesised by using the methods of Collet[21] and Staske and Bohle.[22] Reaction of the amine with 2-, 3-, and 4-pyridinecarboxaldehydes provided the triimine derivatives in good yield, but these compounds proved readily susceptible to hydrolysis making them unsuitable for use as ligands. Interestingly, a salicylylaldehyde derivative reported by Staske and Bohle[22] is stable, as have been other catecholate derivatives prepared by us.[23] The Schiff's base compounds were readily converted to the secondary amines by reduction with $NaBH_4$ to provide compounds **2**–**4** in good yields. The reduction step could be carried out either on the triimine isolated from the reaction as described, or by simply treating the residue isolated by concentrating the reaction mixture with minimal effect on the overall yield.

Crystal structure of $(\mathbf{2})_2\cdot CH_3COCH_3$: Colourless crystals of $(\mathbf{2})_2\cdot CH_3COCH_3$ were isolated by slow evaporation of a solution of **2** in acetone. Compound **2** crystallises in the triclinic space group $P\bar{1}$ with two complete molecules of **2** and an acetone solvate molecule in the asymmetric unit. The two molecules of **2** have quite different orientations of the pyridyl substituents relative to the CTV core; one molecule of **2** has all three pyridyl groups directed above the bowl, while the other has two oriented likewise and a third orthogonal to the veratrole group to which it is attached and pointing downward. These differences in conformation do not significantly alter the packing of the crystallographically unique molecules, which both form a self-clasping dimeric assembly, shown in Figure 1. This motif has previously been observed for other substituted CTG hosts.[5,10,24]

Both self-clasping dimers show edge-to-face π interactions between the pyridyl group within the host cavity and a benzene ring of the CTV bowl ($CH\cdots\pi_{cent}$ distances 2.78 and 2.78 Å; $C\cdots\pi_{cent}$ distances 3.44 and 3.64 Å). This interaction positions the pyridyl group over the centre of the central cyclononane ring, with the nitrogen atom of the pyridine ring orientated out of the cavity. The formation of this self-clasping packing motif precludes the inclusion of solvent molecules within the host cavity. The acetone solvate molecule is

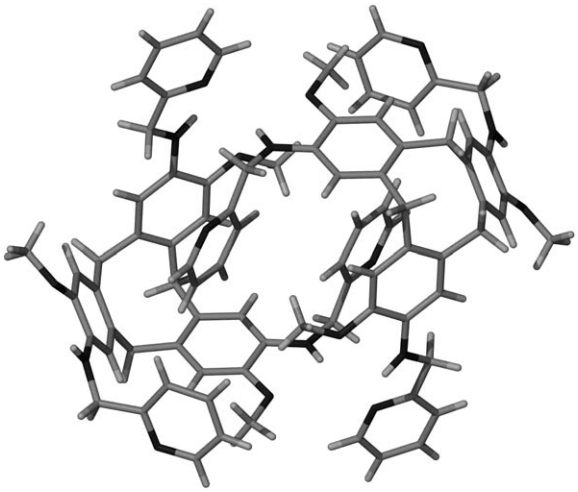

Figure 1. A view of one of the self-clasping dimers of **2** observed within the crystal structure of $(\mathbf{2})_2{\cdot}CH_3COCH_3$.

bound in a general lattice position within the structure. A series of NMR dilution experiments were undertaken on **2** and indicated that no association occurs in acetone.

Crystal Structure of $\mathbf{4}{\cdot}CH_3OH$: Slow evaporation of a solution of **4** in methanol/diethyl ether gives rod-shaped crystals of $\mathbf{4}{\cdot}CH_3OH$ that crystallise in the orthorhombic space group *Pbca*. There is one molecule of **4** and a hydrogen-bonded methanol solvate molecule within the asymmetric unit. Unlike many other extended cavitands in which the predominant orientation of the extended arms is upward to extend the CTV bowl,[5] in this structure two of the three pyridyl groups are directed downwards (Figure 2 (top)). This is in distinct contrast to the conformation the ligand adopts in the complexes and coordination networks described below. The methanol guest hydrogen bonds to one of the downward orientated pyridyl groups (O···N 2.81 Å, O–H···N 1.98 Å).

The 4-pyridyl group that is directed above the cavity is involved in CH···π interactions with the CTV bowl of an adjacent ligand to form an extended structure. This results in the formation of a misaligned columnar stack extending along the *b* axis of the unit cell (Figure 2 (bottom)). The closest distance between the included pyridyl moiety and the lower rim $-(CH_2)_3-$ plane of the host ligand is 4.22 Å. The misaligned self-stacking motif in $\mathbf{4}{\cdot}CH_3OH$ is also observed for α-phase CTV clathrates[1] and other trifunctionalised CTV derivatives.[25]

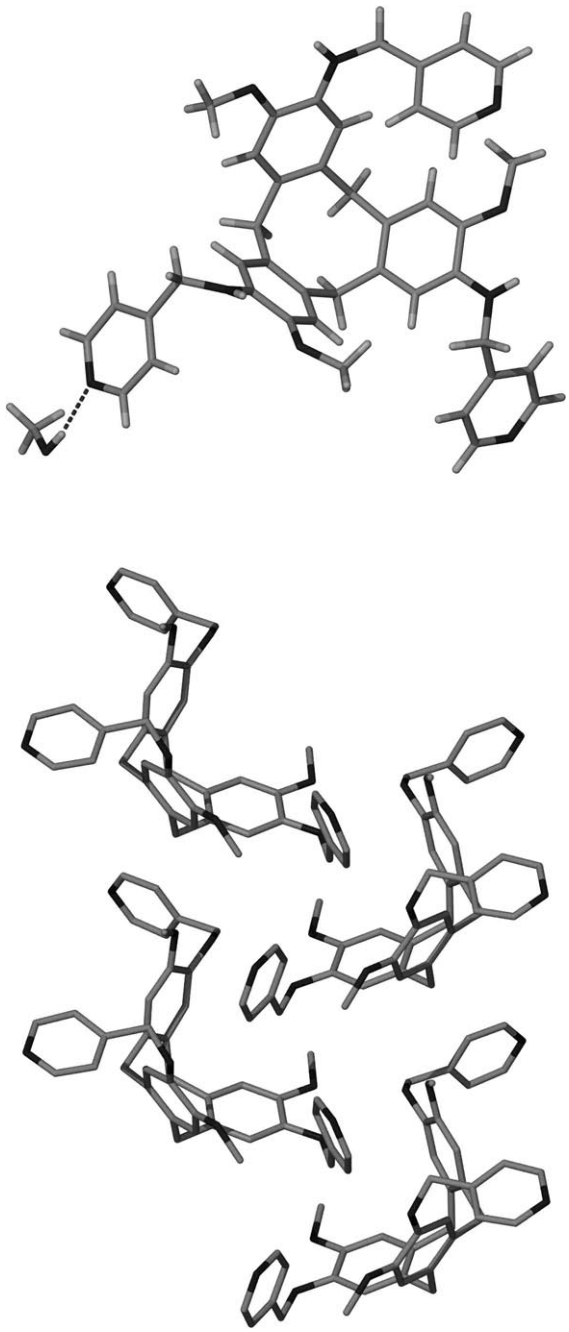

Figure 2. A view of the asymmetric unit (top) and a partial packing diagram (bottom) of the structure of $\mathbf{4}{\cdot}CH_3OH$.

Capsule synthesis, solution studies and X-ray crystallography: We recently reported the formation of a dimeric capsule structure $[Ag_2(\mathbf{3})_2(CH_3CN)_2](PF_6)_2{\cdot}4\,CH_3CN$ that was observed upon reaction of **3** with $AgPF_6$ in a 1:1 stoichiometry.[20] Herein, we describe an investigation of the generality of this structure under various reaction conditions, with other silver salts, and other tetrahedral transition-metal centres. An analogous capsule structure, $[Ag_2(\mathbf{3})_2(CH_3CN)_2][Co(C_2B_9H_{11})_2]_2{\cdot}2\,CH_3CN$ (**5**), was formed from reaction of $Ag[Co(C_2B_9H_{11})_2]$ with cavitand **3**, and the stability and ease of handling of $Ag[Co(C_2B_9H_{11})_2]$ has resulted in it being the first choice for investigation of the affects of stoichiometry. Variation of the $Ag[Co(C_2B_9H_{11})_2]$/ligand stoichiometry from 0.5:1 through to 2:1 led to the observation of essentially the same behaviour in solution and in the solid state. In particular, we could not isolate complexes of other stoichiometry, and increasing the quantity of $Ag[Co(C_2B_9H_{11})_2]$

added simply accelerated the rate of crystallisation of the previously observed $[Ag_2(\mathbf{3})_2]^{2+}$ complex.

As discussed previously,[20] ^{1}H NMR spectroscopy on the complex formed from reaction of $Ag[Co(C_2B_9H_{11})_2]$ with **3** in a 1:1 stoichiometry revealed subtle but significant changes over the ^{1}H NMR spectrum of **3** (Figure 3). In particular,

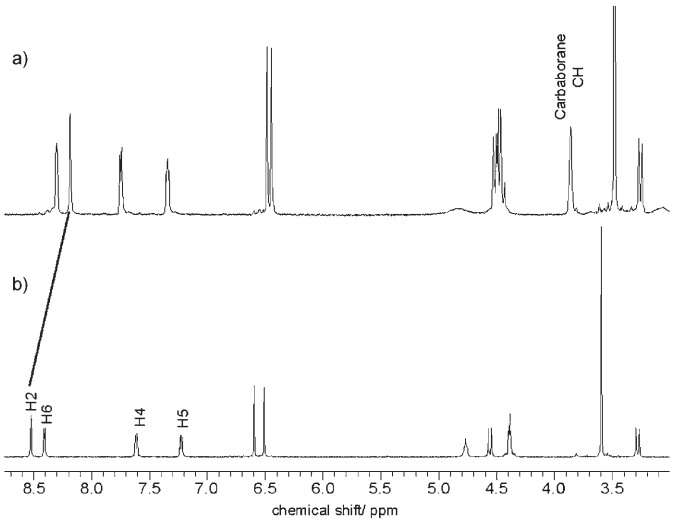

Figure 3. Partial ^{1}H NMR spectra of a) a 1:1 mixture of **3** and $Ag[Co(C_2B_9H_{11})]$ and b) cavitand **3** recorded in $[D_3]$acetonitrile.

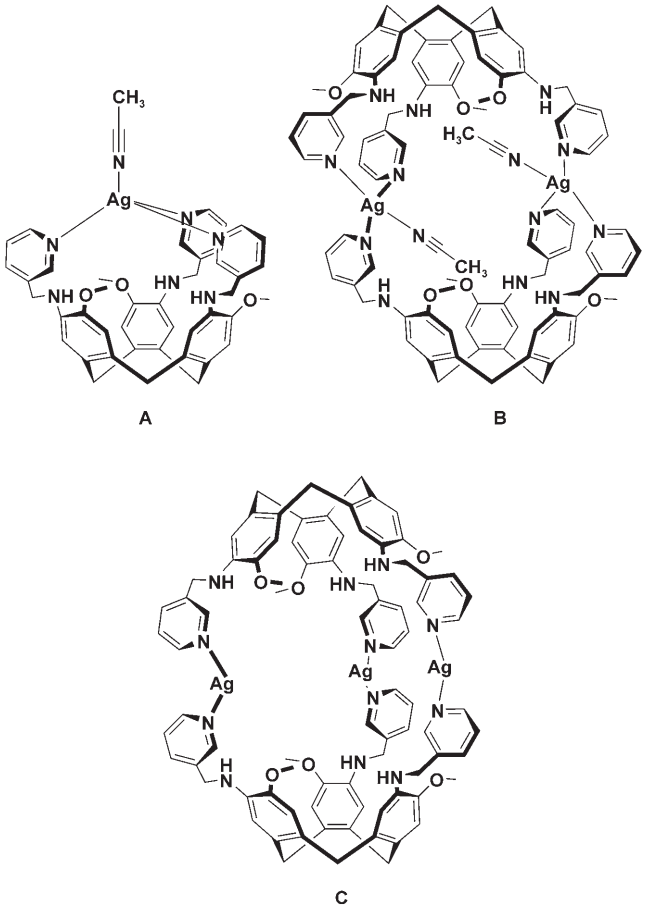

this included the splitting of the signal for the methylene spacer of the pyridyl arms of **3** into two doublets and a considerable upfield shift of the H2 proton of the pyridyl ring, Table 1. This suggested that the pyridyl arms were locked in a defined conformation resulting in internalisation and shielding of the H2 pyridyl proton signal and splitting of the methylene signal. If the $[Ag_2(\mathbf{3})_2(CH_3CN)_2]^{2+}$ capsule is present in solution two sets of signals (in a 2:1 ratio) would be expected. However, only one set of signals is observed for **3** indicating the ligand has C_3 symmetry in solution. This behaviour could result from a number of structures, namely a 1:1 complex (**A**), the $[Ag_2(\mathbf{3})_2]^{2+}$ capsule (**B**) undergoing a rapid exchange process, or an expanded $[Ag_3(\mathbf{3})_2]^{3+}$ cage (**C**). Therefore, unless a fluxional process, which is fast on the NMR timescale, is simplifying the expected spectrum for the $[Ag_2(\mathbf{3})_2]^{2+}$ capsule, then one of the other species, such as the $[Ag_3(\mathbf{3})_2]^{3+}$ cage or an $[Ag(\mathbf{3})]^+$ complex in which the ligand is a tripodal tridentate donor, is present in solution. ES-MS results support the formation of an $[Ag(\mathbf{3})]^+$ complex in solution as no ions of higher molecular mass are observed. In addition, no evidence is observed for the expected encapsulated acetonitrile. Furthermore, addition of other larger nitriles not capable of fitting within the capsule, including benzonitrile and (*S*)-(+)-2-methylbutarynitrile, to the **3**/$Ag[Co(C_2B_9H_{11})_2]$ system has no significant effect on the solution behaviour, indicating that a capsule structure is not likely to be present in solution.

To confirm the type of structure found in solution on reaction of **3** with $Ag[Co(C_2B_9H_{11})_2]$, diffusion-ordered spectroscopy (DOSY)[26–28] was utilised to measure the diffusion coefficients of the cavitand **3** and the solution species formed from **3** and $Ag[Co(C_2B_9H_{11})_2]$ in $[D_6]$acetone. Experimental diffusion rates obtained for two different spherical molecules in the same environment have been shown to be inversely proportional to the ratio of their radii,[29] enabling the relative size of a molecule to be estimated from a comparison of the diffusion rates.[26–28] This has been extended to capsule systems formed from cavitand-based ligands.[28] This is a more direct and broadly applicable method than establishing a Stokes–Einstein relation for this type of system. In this set of experiments $[D_6]$acetone was used, because the capsule structure formed from **3** and $Ag[Co(C_2B_9H_{11})_2]$ rapidly crystallises from acetonitrile. At 291 K, diffusion coefficients (D) of 11.029 ± 0.029 and $10.236 \pm 0.038 \times 10^{-10}$ $m^2 s^{-1}$ were obtained for **3** and a 1:1 mixture of **3** and $Ag[Co(C_2B_9H_{11})_2]$, respectively. The resulting ratio $D_{complex}/D_{ligand}$ is 0.93, which is not in agreement with the theoretical ratio of 0.72–0.75 expected for a dimeric structure.[26,28] The experimental diffusion ratio does support the presence of an $[Ag(\mathbf{3})]^+$ species in acetone. This could be in the form of **3** acting as either a tripodal tridentate donor to the silver centre or as a hypodentate donor, in which the pyridyl groups are made equivalent by a fluxional process. Variation

Table 1. ^{1}H NMR chemical shifts and CIS for reactions of **3** with AgX, $Zn[Co(C_2B_9H_{11})_2]_2$ and $Cu[Co(C_2B_9H_{11})_2]$ in [D_3]acetonitrile or [D_6]acetone.

Compound	H2	H4	H5	H6	Aryl H	Aryl H	NH	CH_2N	CH_2 (i)	CH_2 (o)	OCH_3
3 ([D_3]acetonitrile)	8.54	7.63	7.24	8.42	6.62	6.53	4.78	4.41	4.58	3.30	3.62
+ $Ag[Co(C_2B_9H_{11})_2]$	8.18	7.80	7.40	8.33	6.52	6.48	–	4.52	4.54	3.29	3.51
CIS	*−0.36*	*0.17*	*0.16*	*−0.09*	–	–	–	*0.11*	*−0.04*	*−0.01*	*−0.11*
+ $AgPF_6$	8.15	7.80	7.40	8.42	6.49	6.46	–	4.51	4.53	3.28	3.49
CIS	*−0.39*	*0.17*	*0.16*	*0*	–	–	–	*0.10*	*−0.05*	*−0.02*	*−0.13*
+ $AgBF_4$	8.20	7.78	7.39	8.34	6.51	6.48	4.87	4.51[a]	4.55[a]	3.29	3.51
CIS	*−0.34*	*0.15*	*0.15*	*−0.08*	–	–	–	*0.10*	*−0.03*	*−0.01*	*−0.11*
+ $AgNO_3$	8.24	7.78	7.38	8.35	6.53	6.49	4.87	4.51[a]	4.56[a]	3.29	3.52
CIS	*−0.30*	*0.15*	*0.14*	*−0.07*	–	–	–	*0.10*	*−0.02*	*−0.01*	*−0.10*
+ $Zn[Co(C_2B_9H_{11})_2]_2$	8.27	7.73	7.19	8.20	6.43	6.40	–	4.90/4.56[a]	4.49[a]	3.22	3.51
CIS	*−0.27*	*0.10*	*−0.05*	*−0.22*	–	–	–	*0.49/0.15*	*−0.11*	*−0.08*	*−0.11*
3 ([D_6]acetone)	8.53	7.60	7.15	8.33	6.57	6.52	4.82	4.34	4.55	3.23	3.52
+ $Ag[Co(C_2B_9H_{11})_2]$	8.03	7.80	8.31	8.22	6.52	6.49	–	4.47[a]	4.52[a]	3.14	3.40
CIS	*−0.50*	*0.20*	*0.16*	*−0.11*	–	–	–	*0.13*	*−0.03*	*−0.09*	*−0.12*
+ $AgSbF_6$	8.03	7.89	7.43	8.27	6.52	6.48	–	4.61/4.44[a]	4.47[a]	3.18	3.38
CIS	*−0.50*	*0.29*	*0.28*	*-0.06*	–	–	–	*0.27/0.10*	*−0.08*	*−0.05*	*−0.14*
+ $Ag[Co(C_2B_9H_{11})_2]$ and acetonitrile	7.89	7.84	7.37	8.20	6.51	6.46	–	4.63/4.43[a]	4.47	3.18	3.36
CIS	*−0.64*	*0.24*	*0.22*	*−0.13*	–	–	–	*0.29/0.09*	*−0.08*	*−0.05*	*−0.16*
+ $Ag[Co(C_2B_9H_{11})_2]$ and benzonitrile	8.04	7.92	7.46	8.29	6.57	6.54	–	4.62/4.44[a]	4.48[a]	3.23	3.43
CIS	*−0.49*	*0.32*	*0.31*	*−0.04*	–	–	–	*0.28/0.10*	*−0.07*	*0*	*−0.09*
+ $Ag[Co(C_2B_9H_{11})_2]$ and *S*-(+)-2-methyl-butarynitrile	8.19	7.79	7.32	8.29	6.52	6.52		4.55/4.41[a]	4.51[a]	3.22	3.42
CIS	*−0.34*	*0.29*	*0.17*	*−0.04*	–	–	–	*0.21/0.07*	*−0.04*	*−0.01*	*−0.10*
+ $Cu[Co(C_2B_9H_{11})_2]$	7.90	7.50	7.42	8.09	6.55	6.47	4.92	4.78/4.47[a]	4.47[a]	3.17	3.37
CIS	*−0.63*	*−0.10*	*0.27*	*−0.24*	–	–	–	*0.44/0.13*	*−0.08*	*−0.06*	*−0.15*

[a] Overlapping signals; assignments determined using coupling constants.

in the reaction stoichiometry does affect the resulting $D_{complex}/D_{ligand}$ ratio, which ranges from 0.95 (Ag:L ratio of 0.5:1) to 0.80 (Ag:L ratio of 2:1). This range of values is likely arise from the formation of a number of different species as the amount of $Ag[Co(C_2B_9H_{11})]$ is increased (e.g., capsule-type or polymeric species).

In the solid state acetonitrile appears to play an integral role in templating the formation of the structure; indeed the two specific host–guest interactions observed may be a factor favouring the formation of complex **5**. Thus the diffusion coefficients were also measured in [D_3]acetonitrile with $AgPF_6$ as the metal salt; these conditions gave similar behaviour to that observed in acetone. The diffusion coefficients for this system in [D_3]acetonitrile at 293 K are 11.298 ± 0.037 and $10.469 \pm 0.030 \times 10^{-10}$ $m^2 s^{-1}$ for **3** and a 1:1 mixture of **3** and $AgPF_6$, respectively, resulting in an identical $D_{complex}/D_{ligand}$ ratio of 0.93.

The $D_{complex}/D_{ligand}$ ratios reported above in both acetone and acetonitrile are in good agreement with radii calculations carried out on the crystal structures of the related ligands (**2** and **4**), a 1:1 complex (**A**) and the $[Ag_2(\mathbf{3})_2]^{2+}$ capsule.[30] These calculations have provided approximate radii (r) for **3**, structure **A** and capsule **B** of $r_3 = 5.24$, $r_A = 5.41$ and $r_B = 6.81$ Å, respectively. While the calculations are more valid as the structure under consideration becomes more spherical, the ratios obtained from these calculations lend considerable weight to the given interpretation of the diffusion coefficients. The calculated values for r_A/r_3 is 0.97, which is similar to the experimental value of 0.93. The experimental values differ significantly from the calculated r_B/r_3 ratio of 0.77, which incidentally is in reasonable agreement with other calculated values for the formation of a dimer.[26] This clearly supports the above interpretation of a structure similar to **A** being the observed solution species from reaction of cavitand **3** and AgX.

The $[Ag(\mathbf{3})]^+$ solution species observed for reaction of **3** with $Ag[Co(C_2B_9H_{11})_2]$ or $AgPF_6$ are also observed for reaction of **3** with various other silver salts and transition-metal ions with a tetrahedral coordination geometry. This is demonstrated by a high degree of similarity for the ^{1}H NMR spectra of these reaction mixtures (1:1 stoichiometries) and significant similarities in the CIS (coordination-induced shift; $CIS = \delta_{complex} - \delta_{ligand}$) values, Table 1. Variable-temperature NMR studies on the complexes are unremarkable and show significant broadening of the signals for the $[Ag(\mathbf{3})]^+$ solution species at low temperatures, confirming a degree of fluxionality in the room temperature structure.

It should be noted that, while the solution structures obtained with various transition-metal ions have the same NMR spectra, the solid-state chemistry may be vastly different. In several cases with silver(I) salts, we have obtained the $[Ag_2(\mathbf{3})_2]^{2+}$ capsule in the solid state, but this is not the only structural possibility. Indeed, with $AgSbF_6$ and in the absence of cavity bound guests, a coordination polymer with a 1:1 stoichiometry is obtained as described below. While the solution behaviour of $Cu[Co(C_2B_9H_{11})_2]$ and $Zn[Co(C_2B_9H_{11})_2]_2$ entries (Table 1) follows the expected pattern, we have not obtained single crystals from any copper(I) or zinc(II) reaction.

*Crystal structure of the dimeric capsule $[Ag_2(\mathbf{3})_2(CH_3CN)_2][Co(C_2B_9H_{11})_2]_2 \cdot 2\,CH_3CN$ (**5**)*: The structure of the dimeric $[Ag_2(\mathbf{3})_2]^{2+}$ capsule structure, previously reported as the PF_6^- analogue,[20] will be briefly be reiterated here with the

$[Co(C_2B_9H_{11})_2]^-$ complex **5**. The $[Ag_2(\mathbf{3})_2]^{2+}$ capsule is also obtained with $(CB_{11}H_{12})^-$ and $(CF_3SO_3)^-$ counterions. Complex **5** crystallises in the monoclinic space group $P2_1/n$ with one molecule of **3**, a silver centre, one coordinated and one non-coordinated acetonitrile molecule, and a cobalticarbaborane anion in the asymmetric unit. In the capsule structure, two molecules of **3** are bound in a face-to-face arrangement by two tetrahedral silver atoms (Figure 4). Each silver

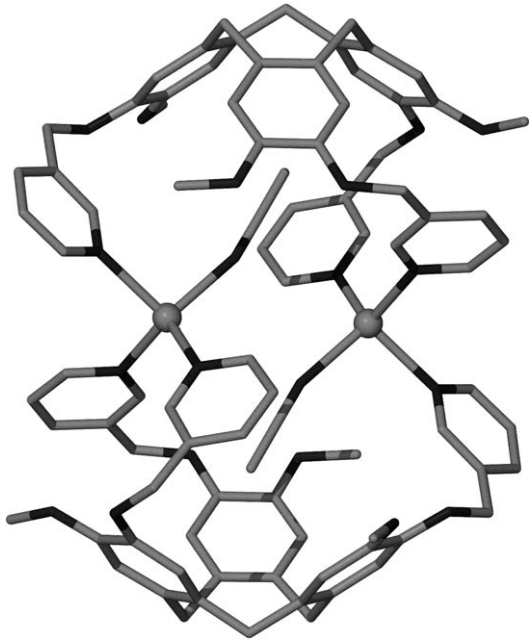

Figure 4. A view of the $[Ag_2(\mathbf{3})_2]^{2+}$ capsule component taken from the crystal structure of **5**. Silver cations are shown in ball and stick representation.

atom is coordinated by two pyridyl groups from one ligand and one pyridyl donor from the second molecule of **3**. A cavity-bound acetonitrile molecule completes the coordination sphere. The Ag–N bond lengths and angles are typical. As expected, almost identical structural parameters are observed for the capsule regardless of the identity of the non-coordinating anion.

Capsulelike structures are not uncommon in the literature with a number examples reported with, typically C_4-symmetric, calixarene and calixresorcinarene cavitands assembled through hydrogen-bonding or coordinate-bonding interactions.[15] An interesting $[Ag_4(L)_2](BF_4)_4$ capsule (in which L is a bipyridyl-substituted resorcinarene cavitand) was recently reported[28] that encapsulates a range of guests including specific hydrogen-bonded heterodimers of a mixture of carboxylic acids. The only other CTV cavitand-based structure reported is a dimeric Pd_3L_2 capsule that has been characterised in solution.[9] This capsule derives from the self-assembly of *cis*-protected Pd units and trisubstituted CTV derivatives possessing rigid pyridyl arms. Covalently linked cryptophanes, in which two CTV fragments are linked in a head-to-head fashion through organic spacers, are well documented.[3] A handful of other $[M_3L_2]$ capsules have been reported that employ a cavitand as the core for the ligand.[13,31–33]

While there are minimal structural differences in the capsule moiety across the range of structures crystallised, the variation of the anion dictates that the different $[Ag_2(\mathbf{3})_2(CH_3CN)_2]X_2$ capsules (in which $X=[Co(C_2B_9H_{11})_2]^-$, complex **5**; $(CB_{11}H_{12})^-$ complex **6**; $(CF_3SO_3)^-$, complex **7**; and PF_6^-, complex **8**[20]) crystallise with different unit cells in different space groups. Complexes **5** and **6** with the larger globular carbaborane anions pack with slightly more open structures ($\rho=1.31$ and 1.35 g cm^{-3}) compared with the two structures formed with $(CF_3SO_3)^-$ and PF_6^- ($\rho=1.43$ and 1.44 g cm^{-3}, respectively). The extended cavitands **2**–**4** are prepared as racemic mixtures and in all structures the two cavitands in each capsule moiety are of opposite hand. Structures **5**, **7** and **8** pack in centrosymmetric space groups, while structure **6** packs in the chiral space group *C*2. The chirality in the last structure arises from the packing of the capsules to form chiral cavities and not directly from the capsules themselves.

*Crystal structure of the coordination polymer {[Ag(**3**)(H$_2$O)](SbF$_6$)}$_n$ (**9**)*: The crystallisation of the $[Ag_2(\mathbf{3})_2(CH_3CN)_2]X_2$ capsule structures described above only occurs from solutions containing acetonitrile. Mixing **3** and $AgSbF_6$ in an acetonitrile/acetone mixture gives an initial oil on evaporation of the solvent, from which crystals of the one-dimensional coordination polymer $\{[Ag(\mathbf{3})(H_2O)](SbF_6)\}_n$ (**9**) form. It is possible the coordination polymer is observed here due to the greater solubility of the SbF_6^-, and the inability of the acetone to coordinate to the silver(I). Complex **9** crystallises in the monoclinic space group *C*2/*c* with one silver atom, one molecule of **3**, a coordinated water molecule and a hexafluoroantimonate anion in the asymmetric unit. The silver atom has a distorted tetrahedral geometry (bond angles in the range 93.56(19) to 137.19(14)°). Three different symmetry-related molecules of **3** (Ag–N bond lengths 2.229(4)–2.333(4) Å) and a water molecule (Ag–O bond length 2.563(6) Å) coordinate each silver cation. In turn, each cavitand **3** coordinates to three silver cations to form a one-dimensional coordination network (Figure 5) of distorted ladder topology.

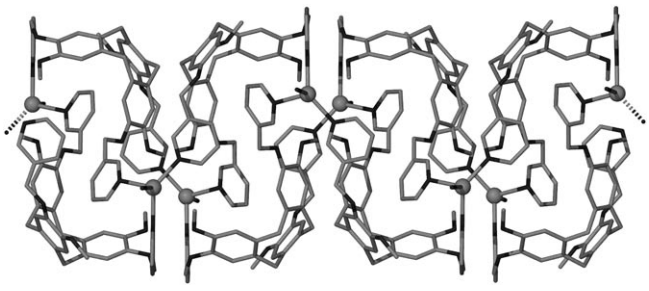

Figure 5. A view of the one-dimensional coordination network in the *bc* plane taken from the crystal structure of $\{[Ag(\mathbf{3})(H_2O)](SbF_6)\}_n$ (**9**). The ligands forming the self-clasping face-to-face units are shown in rod representation and the silver cations in ball and stick representation.

Within the one-dimensional coordination network, pairs of cavitand **3** are involved in self-complementary host–guest interactions, in which one of the pyridyl arms of one molecule of **3** is directed into the cavity of a second cavitand. This results in a "handshake-like" structure in which the two molecules clasp one another. The clasped pyridyl group is located 3.15 Å above the lower rim $-(CH_2)_3-$ plane of the second cavitand, indicating that this is quite an intimate contact. Edge-to-face π interactions between H4 of the included pyridyl group and the benzene ring of the CTV bowl stabilise this arrangement. This clasping face-to-face motif forms a repeating unit within the coordination polymer and prevents the polymeric structure from functioning as a host.

The individual coordination ladders extend down the *c* axis of the unit cell. When viewed in the *bc* plane the undulating nature of the ladders becomes apparent with the pairs of silver atoms connecting the clasping ligands arranged in a zigzag pattern (Figure 5). The overall crystal packing of **9** shows the SbF_6^- counterions arranged within cavities created by the packing of the one-dimensional coordination polymers. These are located within hydrogen-bonding distances of the coordinated water molecules (O–H···F distance of 2.76 Å). The crystal packing also reveals π-stacking interactions[34] between CTV cores of adjacent polymers (centroid–centroid distances of 3.96 Å).[35]

The coordination polymer described here bears a close structural resemblance to the $[Ag_2(\mathbf{3})_2]X_2$ capsule structures typically formed with this ligand. In fact on a gross level, the capsule and polymeric structures are related simply by a change in the orientation of one of the pyridyl groups that allows it to coordinate to the silver cation of an adjacent clasped cage structure. This is somewhat akin to the ring opening polymerisation of cages observed for other labile transition-metal systems.[36] It is pertinent to note, however, that the polymer and the closest related capsule structure are formed with different octahedral anions, namely SbF_6^- and PF_6^- respectively, and additionally, that the capsule structure is not likely to be a precursor to the polymer as it is not observed in solution. Therefore, while the compounds bear a close structural relationship, they are not precursor and polymer in the sense invoked above. It is more likely that a dimerisation pathway is in equilibrium with a polymerisation process in this system. It is also well established that changes in the anion affect the type of structure observed with multidentate ligands and transition metals.[37]

Synthesis of stellated tetrahedral prisms, solution studies and X-ray crystallography: The synthesis and crystal structure of an $[Ag_4(\mathbf{4})_4]^{4+}$ tetrahedral prismatic cage has been previously described with cavitand **4**.[20] This structure was initially reported with tetrafluoroborate as the anion; herein we describe similar structures with $AgPF_6$ (complex **10**) and $AgSbF_6$ (complex **11**). The synthesis of the $[Ag_4(\mathbf{4})_4]^{4+}$ cage structure is straightforward; simply combining solutions of **4** and AgX in acetonitrile leads to its formation.

Unlike the dimeric capsule structure described above that is only formed upon crystallisation, the $[Ag_4(\mathbf{4})_4](PF_6)_4$ prism **10** appears to be present in solution. ^{1}H NMR spectroscopy on a 1:1 mixture of $AgPF_6$ and **4** reveals a number of significant changes over the ^{1}H NMR spectrum of **4** only. In the solution species the NMR signals are consistent with the cavitand possessing C_3 symmetry as expected for **10** in solution. In addition, coordination-induced shifts are observed for a number of signals at room temperature, and more noticeably at low temperature, in particular for those protons located around the middle band of the cavitand, as listed in Table 2. These are particularly noteworthy for the pyridyl H3/H5, aryl, NH, and OCH_3 protons of **4**, which on forming the $[Ag_4(\mathbf{4})_4](PF_6)_4$ tetrahedral prism are located in the shielding regions of nearby aromatic rings. The coordination to the silver atom by the pyridyl nitrogen atom probably counteracts the shielding effects experienced by the pyridyl H2/H6 protons. At room temperature some of the signals for **10** are broadened, but upon cooling these sharpen and the shifts arising from coordination become more dramatic (Figure 6).

Further support for a tetrameric structure in solution also comes from DOSY NMR measurements made under the regime described for the capsule. This provided diffusion coefficients of 11.217 ± 0.034 and $7.633 \pm 0.071 \times 10^{-10}\,m^2 s^{-1}$ for **4** and a 1:1 mixture of **4** and $AgPF_6$, respectively, at 293 K, giving qualified support for a tetramer. The resulting ratio $D_{complex}/D_{ligand}$ is 0.68 putting it lower than the ratio expected for a dimer[26,28] and in the range expected for larger species.[26] Literature $D_{trimer}/D_{monomer}$ ratios for hard sphere contacts of equilateral trimers are 0.62–0.66. Suitable values for comparison are difficult to locate, as this approach to interpreting diffusion rates has been mainly directed toward the consideration of assemblies of spherical monomers[26] and rarely extended beyond dimers in metallo-supramolecular chemistry. A comparison with the ratio of the radii for the tetramer and cavitand **4** calculated from the crystal structures ($D_{complex}/D_{ligand} = 0.60$) provide a value lower than that obtained experimentally. Thus in summary, the experimental $D_{complex}/D_{ligand}$ ratio of 0.68 indicates a species of large size (trimer or tetramer) is present in solution, but they cannot be distinguished by this approach. Nonetheless, the $D_{complex}/D_{ligand}$ ratios obtained for increasing amounts of added

Table 2. ^{1}H NMR chemical shifts for **4** and **10** and CIS for **10** in [D$_3$]acetonitrile.

Compound	H2/H6	H3/H5	Aryl H	Aryl H	NH	CH_2N	CH_2(i)	CH_2(o)	OCH_3
4 (243 K)[a]	8.43	7.17	6.44	6.35	5.05	4.44	4.44	3.19	3.35
+ $AgPF_6$ (233 K)	8.31	6.74	6.21	6.18	3.53	4.65/4.30	4.30	3.10	2.88
CIS	*−0.12*	*−0.43*	*−0.23*	*−0.17*	*−1.52*	*0.21/−0.14*	*−0.14*	*−0.09*	*−0.47*

[a] ^{1}H NMR spectrum of **4** recorded at 243 K as sample solidifies at 233 K.

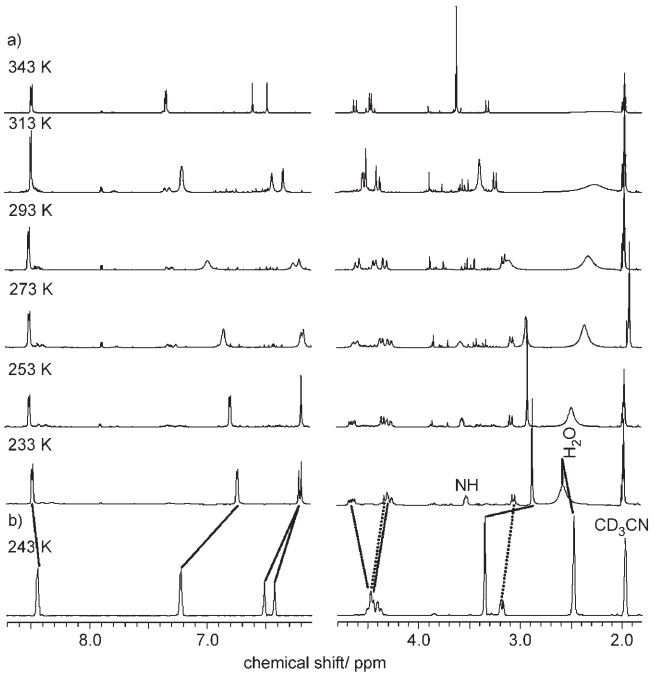

Figure 6. a) Partial ^{1}H NMR spectra obtained for compound **10** in [D_3]acetonitrile at temperatures between 233 and 343 K and b) partial ^{1}H NMR spectrum for cavitand **4** at 243 K. Lines highlight the significant coordination-induced shifts observed for **10** at low temperatures.

$AgPF_6$ are similar to that obtained for the 1:1 stoichiometry, indicating that the species observed is likely to be the most stable and largest structure present. Conclusive support for a tetrameric structure comes from MALDI mass spectrometry, which shows a doubly charged ion with a m/z ratio of 1718.2. This is consistent with the intact $[Ag_4(\mathbf{4})_4]$ prism less two PF_6^- counterions.

The stability of the $[Ag_4(\mathbf{4})_4](PF_6)_4$ prism in solution over the dimeric capsule structure can be readily understood in terms of a mechanical interlocking of the tetrahedral species. The $[Ag_2(\mathbf{3})_2]^{2+}$ capsule structure is a much more open structure that can undergo significant reorganisation around the silver cation upon the disconnection of one Ag–N_{py} bond. This readily allows for the formation of other species in solution. In contrast the $[Ag_4(\mathbf{4})_4]^{4+}$ prism is a rigid and interlocked structure that cannot be opened up to solvolysis by acetonitrile through simply cleaving one Ag–N_{py} bond. The pyridyl nitrogen donor is held rigidly in place by the other two Ag–N_{py} bonds of the cavitand.

*Crystal structures of $[Ag_4(\mathbf{4})_4(CH_3CN)_3]\cap(CH_3CN)_4(PF_6)_4\cdot 9.5\,CH_3CN\cdot 0.5\,H_2O$ (**10**) and $[Ag_4(\mathbf{4})_4(CH_3CN)_3]\cap(CH_3CN)_4(SbF_6)_4\cdot 5\,CH_3CN$ (**11**)*: The crystal structures of **10** and **11** show only subtle differences from the BF_4^- analogue described by us in a recent communication.[20] Crystals of compound **10** were obtained by vapour diffusion of diethyl ether into a solution of $AgPF_6$ and **4** in a 1:1 stoichiometric proportion in acetonitrile. This yielded poorly diffracting colourless crystals with the formulation $[Ag_4(\mathbf{4})_4(CH_3CN)_3]\cap(CH_3CN)_4(PF_6)_4\cdot 9.5\,CH_3CN\cdot 0.5\,H_2O$ (**10**) that crystallised in the monoclinic space group $P2_1/c$. A better data set was obtained using synchrotron radiation for the SbF_6 analogue **11**, which was crystallised by vapour diffusion of diethyl ether into a solution containing $AgSbF_6$ and **4** in a 1:1 ratio in acetonitrile/2,2,2-trifluoroethanol. This structure, with the formulation $[Ag_4(\mathbf{4})_4(CH_3CN)_3]\cap(CH_3CN)_4(SbF_6)_4\cdot 5\,CH_3CN$, also crystallises in the monoclinic space group $P2_1/c$ and is outlined briefly below.

Similar to the previously reported $AgBF_4$ structure, complex **11** has the structure of a stellated tetrahedral prism (Figure 7) that serves as a host for five acetonitrile guest molecules (one coordinated to a silver cation of the cage). The four crystallographically independent silver cations have either trigonal planar three-coordinate geometries coordinated by pyridyl groups from three different molecules of **4** (Ag4), or distorted trigonal pyramidal four-coordinate geometries formed from three pyridyl donors and supplemented by an acetonitrile ligand (Ag1, Ag2 and Ag3). One of the silver centres, Ag1, has the terminal acetonitrile directed into the prism at a distance of 2.67(2) Å and also makes a long contact with a fluorine atom of an SbF_6^- ion (Ag–F distances of 2.88(3) Å).

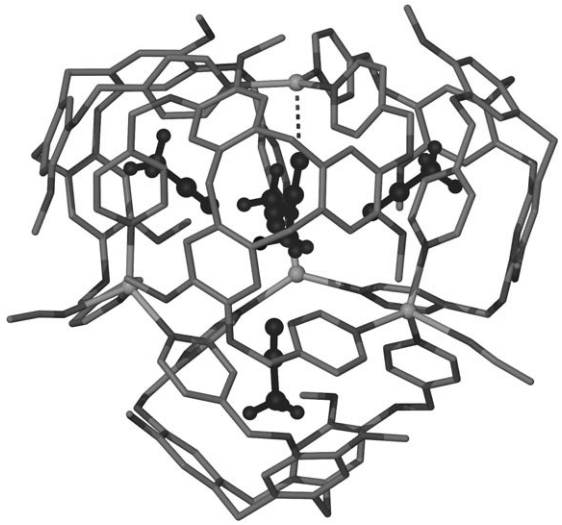

Figure 7. A view of a $[Ag_4(\mathbf{4})_4(CH_3CN)_3]\cap(CH_3CN)_4$ stellated tetrahedron taken from the structure of **11**, with the silver cations and acetonitrile molecules within the tetrahedron shown in ball and stick representation.

Tetrahedral metallo-supramolecular prisms are not uncommon, but examples possess either an $[M_4L_6]$ stoichiometry in which the six ligands define the edges of the tetrahedron or an $[M_4L_4]$ composition with C_3-symmetric tritopic ligands.[38–40] The former category represents a significant proportion of these structures that continue to stimulate interest.[41] Indeed, a recent communication by Ward and coworkers reported the diastereoselective formation of an $[M_4L_6]$ tetrahedral cage using a chiral pyridyl–pyrazole ligand.[42] The most closely related structures to the $[Ag_4(\mathbf{4})_4]$ tetrahedra are an $[Mn_4L_4]$ tetrahedron with a podand borate ligand,[38] and a $[Cu_8L_4]$ tetrahedral structure, in which the

calixresorcinarene ligands act as the vertices of a metallo-supramolecular tetrahedron.[16] The $[Cu_8L_4]$ tetrahedron has large triangular windows with dimensions of approximately 14 Å, whereas the stellated tetrahedron reported here has virtually no portals for the exchange of guest molecules.

Recently, Raymond et al. reported the formation of large $[M_4L_4]$ tetrahedra following an extension of their symmetry-based design approach using planar ligands with catechol donor functionalities.[43] This approach to increasing the internal dimensions of $[M_4L_4]$ tetrahedra has also been described by Albrecht et al.[40] These structures are of similar dimensions to the stellated tetrahedron. Raymond and coworkers noted that increased conformational flexibility of the ligands somewhat limits the quest for structures with larger internal cavities. Using cavitands, such as those reported here and by Beer et al., presents a further approach to increase the internal volume of an $[M_4L_4]$ tetrahedron possibly without the penalties of further conformational mobility—the cavitand provides intrinsic additional internal volume.

*Crystal structures of the coordination polymers {[Ag(**4**){N≡C(CH$_2$)$_3$C≡N}]∩(N≡C(CH$_2$)$_3$C≡N)PF$_6$}$_n$ (**12**) and {[Ag(**4**)-{N≡C(CH$_2$)$_3$C≡N}]∩(N≡C(CH$_2$)$_3$C≡N)[Co(C$_2$B$_9$H$_{11}$)$_2$]·N≡C-(CH$_2$)$_3$C≡N}$_n$ (**13**)*: Under our research program, considerable effort is directed toward the preparation of cavitand-based coordination networks.[5,11] The stellated tetrahedral prisms described above with their exchangeable terminal acetonitrile ligands represent ideal building blocks from which to assemble infinite coordination networks. Thus we treated the cage-forming components **4** and AgX with the dinitriles succinonitrile and glutaronitrile. From a mixture of the latter dinitrile, **4** and $AgPF_6$, we obtained pale brown, rod-shaped crystals of **12** on slow evaporation of the acetonitrile solvent medium. Use of $Ag[Co(C_2B_9H_{11})_2]$ in place of $AgPF_6$ provided yellow needle-shaped crystals of **13**, which crystallised from an acetonitrile and 2,2,2-trifluoroethanol solvent mixture. The structures of both **12** and **13** were determined by X-ray crystallography to reveal that the desired tetrahedral prismatic structural motif was not maintained and had been disrupted by the larger glutaronitrile guest molecule resulting in the formation of a 4.8^2 two-dimensional network structure. This demonstrates an interesting interplay between the discrete tetrameric structure and an infinite coordination network. The crystallographic details of compound **12** are given in the Supporting Information, while structure **13** is described below. Compound **13** crystallises in the monoclinic space group *C*2/*c* with an asymmetric unit containing one silver atom, one molecule of **4**, three glutaronitrile moieties (one coordinated, one bound within the cavity of **4** and the third in the channels within the structure), and a cobalticarbaborane counterion (Figure 8).

Within the extended structure both the silver cations and the cavitand are three-connecting nodes. The silver has a tetrahedral geometry coordinated by three pyridyl moieties from three different molecules of **4** ($Ag-N_{py}$ bond lengths of 2.343(6)–2.369(6) Å) and a monodentate capping glutaronitrile molecule (Ag–N bond length of 2.25(1) Å). The three cavitands coordinating to each silver centre are orientated such that two have the top face orientated in the same direction with the third directed in an opposing direction. The cavitand is likewise coordinated to three different symmetry-related silver cations and acts as a host for the second molecule of glutaronitrile. Overall this results in a 4.8^2 two-dimensional network structure that extends along the *bc* plane of the unit cell (Figure 9).

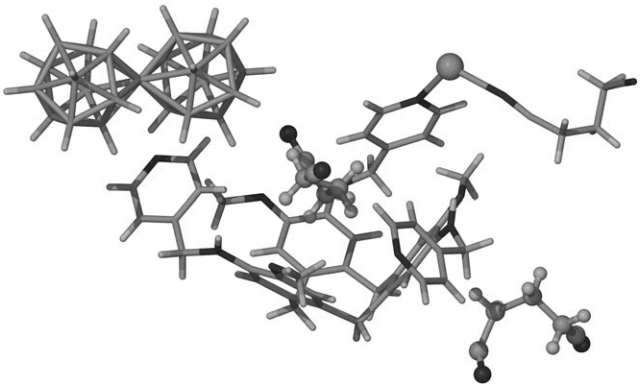

Figure 8. A view of the asymmetric unit of the crystal structure of **13**, showing the host–guest interaction between **4** and glutaronitrile. The silver atom, the guest glutaronitrile molecule and a channel-included glutaronitrile molecule are shown in ball and stick representation.

The glutaronitrile guest is orientated such that the more hydrophobic aliphatic chain of the molecule is directed into the cavity. The distances from the two closest aliphatic carbon atoms to the centroid of the $-(CH_2)_3-$ moiety of **4** are 4.11 and 4.79 Å, which indicate that the guest molecule is perched over the cavity rather than extending into it. The glutaronitrile guest molecule acts as a hydrogen-bond acceptor for an NH proton of **4** (N–H···N≡C distance of 2.57 Å). This results in a dimeric motif in which the cavitand that provided the NH proton is in turn a host for a glutaronitrile molecule that forms a reciprocal interaction.

The overall structure results from layering of the undulating two-dimensional 4.8^2 networks within the crystal to form an extended network structure incorporating roughly rectangular channels (Figure 10). In compound **13** these channels are largely occupied by the globular cobalticarbaborane anions and glutaronitrile molecules and are effectively blocked. The remaining "voids" within the channels contains residual electron density that was not modelled.

In comparison with structure **13**, the channels in **12** appear more open because they contain the smaller hexafluorophosphate anions. However, the channels are of course not empty and the Fourier difference map reveals they still contain considerable residual electron density that could not be adequately modelled as solvent or glutaronitrile molecules. The contents of these channels are significantly disordered and thus it is possible to envisage removal and exchange of these molecules. The roughly rectangular-shaped channels, with approximate dimensions of 13.6 by 9.2 Å, project a generally hydrophobic surface as they are

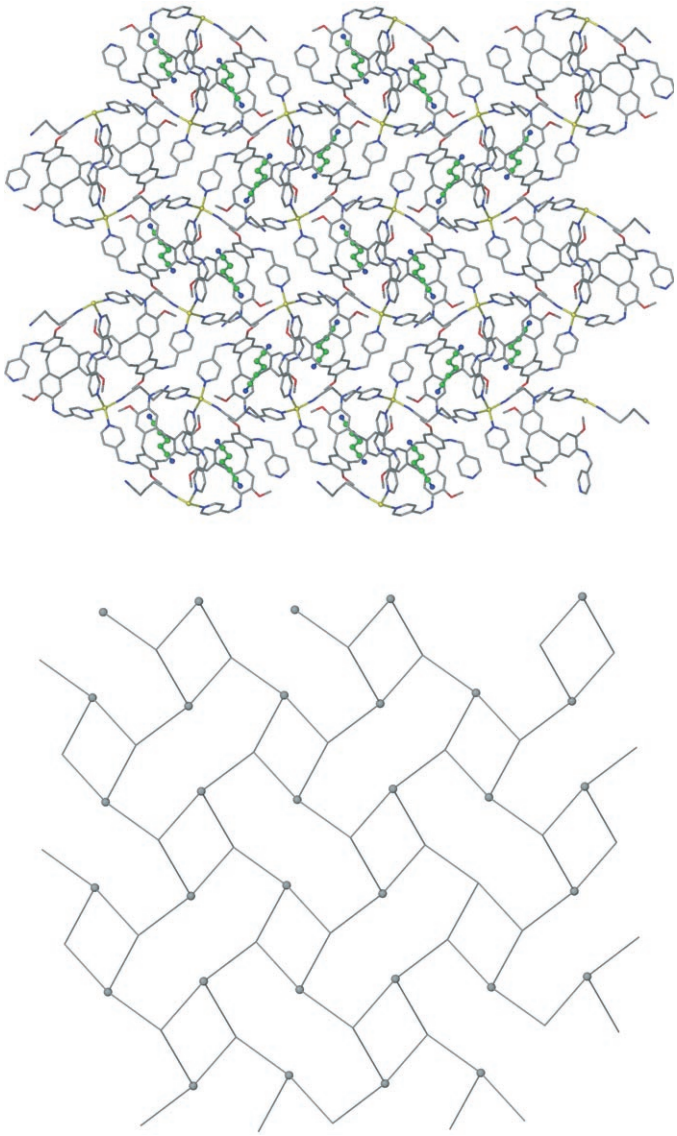

Figure 9. Views of the crystal structure of **13** looking down on the *bc* plane of the extended 4.8^2 two-dimensional network structure (top) and a topological diagram illustrating the connectivity between the silver atoms and the centroids of **4** (bottom). Silver centres and guest glutaronitrile molecules are shown in ball and stick representation.

lined with aryl rings from the CTV bowl of the cavitands and coordinated glutaronitrile species that project into the channel. The PF_6^- counterions are nestled in the sides of the channel, as shown in Figure 10 (bottom).

In summary, we have undertaken an investigation of the solution and solid-state behaviour of two discrete metallo-supramolecular polyhedra formed from late transition-metal ions and trimeric CTV-based cavitands. DOSY NMR measurements in conjunction with other NMR data have revealed that the dimeric $[Ag_2(\mathbf{3})_2(CH_3CN)_2]^{2+}$ capsule is not observed in solution, but that the $[Ag_4(\mathbf{4})_4]^{4+}$ tetrahedron is likely to be present in solution. A proposed monomeric $[Ag(\mathbf{3})]^+$ species can dimerise to form the observed $[Ag_2(\mathbf{3})_2(CH_3CN)_2]^{2+}$ capsule structures or polymerise, in

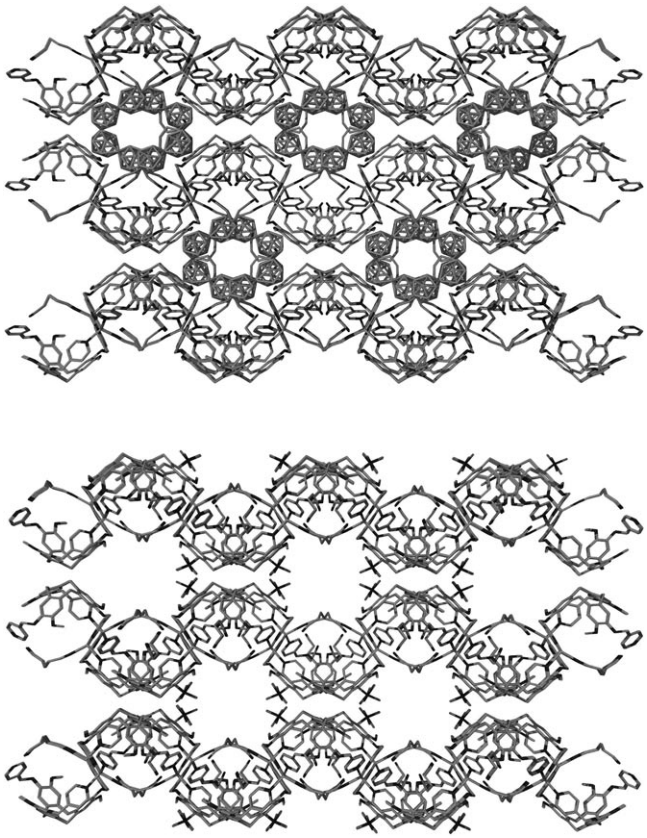

Figure 10. Partial packing diagrams of the crystal structures of **13** (top) and **12** (bottom) looking down the *c* axis of the unit cell and three of the layered 4.8^2 two-dimensional coordination networks. The large channels that extend down the *c* axis of the unit cell contain the anions and lattice-included glutaronitrile molecules.

the absence of an acetonitrile template, to provide a one-dimensional coordination polymer in the case of $AgSbF_6$. In the presence of acetonitrile, $[Ag_4(\mathbf{4})_4]^{4+}$ tetrahedra are formed with a range of anions, but a larger dinitrile guest, glutaronitrile, disrupts the formation of this cage structure resulting in the formation of 4.8^2 network structures, **12** and **13**. We have aptly demonstrated that we can control the self-assembly pathway and the interplay of discrete metallo-supramolecular species and infinite coordination networks in our trimeric cavitand ligand systems through host–guest interactions.

Experimental Section

General experimental: Melting points were recorded on a Bibby melting point apparatus and are uncorrected. The University of Leeds microanalytical laboratory performed elemental analyses on samples that were dried in vacuo for several hours. Electrospray (ES) mass spectra were collected at the University of Leeds using a Micromass LCT mass spectrometer and MALDI mass spectra at the EPSRC National Mass Spectrometry Service Centre in Swansea. Unless otherwise stated, reagents were obtained from commercial sources and used as received. The following compounds were prepared by literature procedures: 4-amino-3-methoxybenzyl alcohol,[21] 4-acetamido-3-methoxybenzyl acetate,[21] (±)-

3,8,13-triacetamido-2,7,12-trimethoxy-10,15-dihydro-5*H*-tribenzo-[*a*,*d*,*g*]cyclononene,[21] (±)-3,8,13-triamino-2,7,12-trimethoxy-10,15-dihydro-5*H*-tribenzo[*a*,*d*,*g*]cyclononene trihydrochloride (**1**·3HCl),[22] and (±)-3,8,13-triamino-2,7,12-trimethoxy-10,15-dihydro-5*H*-tribenzo-[*a*,*d*,*g*]cyclononene (**1**).[22]

NMR studies: NMR spectra were recorded on a Bruker 250 MHz or 500 MHz spectrometers by using a 5 mm probe at 300 K unless otherwise stated. NMR solutions of the complexes were prepared as required by dissolving the appropriate ligand (typically 5 mg, 7.4 μmol) and metal salt (7.4 μmol) in deuterated solvent (ca. 600 μL).

DOSY NMR measurements: DOSY NMR measurements were made on a Varian Inova 500 MHz spectrometer operating either without temperature control (measurements in [D$_6$]acetone) or under regulated temperature conditions (20 °C, measurements in [D$_3$]acetonitrile), with a 5 mm probe. The pulse sequence employed was a bipolar pulse pair simulated echo (BPPSTE)[44] operating in the ONESHOT experiment.[45] Additional parameters: number of different gradient levels, 20; gradient stabilisation delay, 0.002 s; gradient length, 0.0025 s; diffusion delay, 0.03 s; relaxation delay, 10 s; Kappa (unbalancing factor), 0.2. Spectra were recorded for 5 mM solutions of ligand with added AgX (0.5, 1.0, 1.5 and 2.0 equivalents).

Ligand synthesis—general method

Part A: The amine hydrochloride **1**·3HCl (1 mmol), the requisite pyridine carboxyaldehyde (3.1 mmol), triethylamine (2 mL) and ethanol (60 mL) were heated to reflux for 3 h. The reaction mixture was cooled to room temperature and the solvent removed in vacuo to give the bright yellow triimine derivatives. This solid can either be used in part B without further purification (typical route), or triturated with methanol, collected by filtration, washed with ice-cold methanol, then diethyl ether, and dried under vacuum to give a fluffy yellow solid. These triimine derivatives decompose in solution over a period of minutes to hours and as a solid over a period of hours to days.

Part B: The triimine derivative was dissolved in a 1:1 mixture of dichloromethane and ethanol (60 mL) and sodium borohydride (excess) was added in small portions. The reaction mixture stirred at room temperature for 96 h. The solvent was removed in vacuo and the solid was taken up in dichloromethane (150 mL); the chlorinated extract was washed with water (50 mL) and brine (50 mL), and then was dried over magnesium sulfate. The solvent was removed and the resulting oily solids were purified by chromatography on silica gel using 5% methanol in dichloromethane (+ five drops triethylamine per 100 mL) as the eluent. The off-white solid obtained was suspended in methanol, filtered, washed with further portions of cold methanol and dried under vacuum.

(±)-2,7,12-Trimethoxy-3,8,13-tris(2-pyridylmethylamino)-10,15-dihydro-5*H*-tribenzo[*a*,*d*,*g*]cyclononene (2)

Part A: Yield: 70%; ^{1}H NMR (CDCl$_3$): δ=3.72 (d, J=13.7 Hz, 3H; CH_2), 3.87 (s, 9H; OCH_3), 4.85 (d, J=13.7 Hz, 3H; CH_2), 6.96 (s, 3H; aryl C*H*), 7.16 (s, 3H; aryl C*H*), 7.34 (dd, J=4.8, 7.5 Hz, 3H; pyH5), 7.78 (t, J=7.8 Hz, 3H; pyH4), 8.22 (d, J=7.8 Hz, 3H; pyH3), 8.63 (s, 3H; NC*H*py), 8.69 ppm (d, J=4.2 Hz, 3H; pyH6). No further characterisation was undertaken as this compound decomposes slowly in solution and the solid state.

Part B: Yield: 80%; m.p. 149–51 °C; ^{1}H NMR (CDCl$_3$): δ=3.27 (d, J=13.7 Hz, 3H; CH_2), 3.55 (s, 9H; OCH_3), 4.41 (s, 6H; NHCH_2py), 4.57 (d, J=13.7 Hz, 3H; CH_2), 4.76 (br s, 3H; N*H*), 6.35 (s, 3H; aryl C*H*), 6.42 (s, 3H; aryl C*H*), 7.08 (dd, J=5.2, 7.2 Hz, 3H; pyH5), 7.27 (d, J=7.7 Hz, 3H; pyH3), 7.52 (t, J=7.7 Hz, 3H; pyH4), 8.50 ppm (d, J=4.2 Hz, 3H; pyH6); ^{1}H NMR ([D$_6$]acetone): δ=3.25 (d, J=13.6 Hz, 3H; CH_2), 3.58 (s, 9H; OCH_3), 4.35 (s, 6H; NHCH_2py), 4.57 (d, J=13.4 Hz, 3H; CH_2), 5.15 (br s, 3H; N*H*), 6.50 (s, 3H; aryl C*H*), 6.62 (s, 3H; aryl C*H*), 7.12 (dd, J=4.9, 6.5 Hz, 3H; pyH5), 7.23 (d, J=7.8 Hz, 3H; pyH3), 7.56 (t, J=7.7 Hz, 3H; pyH4), 8.45 ppm (d, J=4.7 Hz, 3H; pyH6); ^{13}C NMR (CDCl$_3$): δ=36.87, 50.08, 56.02, 111.68 (two overlapping signals), 121.50, 122.26, 128.54, 132.79, 136.69, 137.17, 146.01, 149.50, 160.34 ppm; ^{13}C NMR ([D$_6$]acetone): δ=37.20, 50.29, 56.46, 112.51, 112.64, 122.37, 123.10, 129.10, 133.94, 137.69, 137.78, 146.85, 150.25, 161.17 ppm; HRMS (ES+): calcd for $C_{42}H_{43}N_6O_3^+$: 679.3397; found: 679.3386; elemental analysis calcd (%) for $C_{42}H_{42}N_6O_3\cdot1.75H_2O$: C 71.00, H 6.47, N 11.83; found: C 71.05, H 6.35, N 11.55.

(±)-2,7,12-Trimethoxy-3,8,13-tris(3-pyridylmethylamino)-10,15-dihydro-5*H*-tribenzo[*a*,*d*,*g*]cyclononene (3)

Part A: Yield: 95%; ^{1}H NMR (CDCl$_3$): δ=3.72 (d, J=13.6 Hz, 3H; CH_2), 3.85 (s, 9H; OCH_3), 4.84 (d, J=13.7 Hz, 3H; CH_2), 6.96 (s, 3H; aryl C*H*), 7.07 (s, 3H; aryl C*H*), 7.39 (dd, J=4.7, 7.5 Hz, 3H; pyH5), 8.29 (d, J=7.9 Hz, 3H; pyH4), 8.48 (d, J=7.2 Hz, 3H; pyH6), 8.69 (d, J=4.7 Hz, 3H; pyH3), 8.95 ppm (s, 3H; NC*H*py). No further characterisation was undertaken as this compound decomposes slowly in solution and the solid state.

Part B: Yield: 71%; m.p. 204–5 °C; ^{1}H NMR (CDCl$_3$): δ=3.29 (d, J=13.7 Hz, 3H; CH_2), 3.54 (s, 9H; OCH_3), 4.28 (s, 6H; NHCH_2py), 4.60 (d, J=13.7 Hz, 3H; CH_2), 6.36 (s, 3H; aryl C*H*), 6.42 (s, 3H; aryl C*H*), 7.16 (dd, J=4.7, 7.7 Hz, 3H; pyH5), 7.60 (d, J=7.8 Hz, 3H; pyH4), 8.43 (d, J=4.7 Hz, 3H; pyH6), 8.55 ppm (d, J=1.8 Hz, 3H; pyH2), NH proton not observed; ^{1}H NMR (CD$_2$Cl$_2$): δ=3.25 (d, J=13.5 Hz, 3H; CH_2), 3.54 (s, 9H; OCH_3), 4.27 (br s, 6H; NHCH_2py), 4.43 (br s, 3H; NH), 4.55 (d, J=13.5 Hz, 3H; CH_2), 6.36 (s, 3H; aryl C*H*), 6.44 (s, 3H; aryl C*H*), 7.14 (dd, J=4.8, 7.8 Hz, 3H; pyH5), 7.57 (d, J=7.9 Hz, 3H; pyH4), 8.39 (d, J=4.7 Hz, 3H; pyH6), 8.51 ppm (d, J=1.6 Hz, 3H; pyH2); ^{1}H NMR ([D$_6$]acetone): δ=3.23 (d, J=13.6 Hz, 3H; CH_2), 3.51 (s, 9H; OCH_3), 4.34 (br s, 6H; NHCH_2py), 4.55 (d, J=13.5 Hz, 3H; CH_2), 4.85 (br s, 3H; NH), 6.52 (s, 3H; aryl C*H*), 6.57 (s, 3H; aryl C*H*), 7.16 (dd, J=4.7, 7.8 Hz, 3H; pyH5), 7.60 (d, J=7.8 Hz, 3H; pyH4), 8.33 (d, J=4.6 Hz, 3H; pyH6), 8.53 ppm (d, J=1.5 Hz, 3H; pyH2); ^{1}H NMR (CD$_3$CN): δ=3.28 (d, J=13.6 Hz, 3H; CH_2), 3.59 (s, 9H; OCH_3), 4.39 (t, J=5.3 Hz, 6H; NHCH_2py), 4.56 (d, J=13.6 Hz, 3H; CH_2), 4.80 (t, J=5.2 Hz, 3H; NH), 6.51 (s, 3H; aryl C*H*), 6.59 (s, 3H; aryl C*H*), 7.23 (dd, J=4.7, 7.7 Hz, 3H; pyH5), 7.61 (d, J=7.8 Hz, 3H; pyH4), 8.41 (d, J=3.8 Hz, 3H; pyH6), 8.52 ppm (d, J=1.4 Hz, 3H; pyH2); ^{13}C NMR (CDCl$_3$): δ=35.51, 44.72, 54.53, 110.19 (2 overlapping signals), 122.64, 127.37, 131.36, 133.99, 134.57, 135.23, 144.55, 147.39, 147.60 ppm; ^{13}C NMR (CD$_2$Cl$_2$): δ=37.00, 46.41, 56.35, 111.86, 111.96, 124.22, 128.89, 133.10, 135.39, 136.27, 137.22, 146.44, 149.27, 149.69 ppm; HRMS (ES+): calcd for $C_{42}H_{43}N_6O_3^+$: 679.3397; found: 679.3406; elemental analysis calcd (%) for $C_{42}H_{42}N_6O_3\cdot0.5H_2O$: C 73.33, H 6.31, N 12.22; found: C 73.60, H 6.35, N 12.05.

(±)-2,7,12-Trimethoxy-3,8,13-tris(4-pyridylmethylamino)-10,15-dihydro-5*H*-tribenzo[*a*,*d*,*g*]cyclononene (4)

Part A: Yield: 76%; ^{1}H NMR (CDCl$_3$): δ=3.72 (d, J=13.7 Hz, 3H; CH_2), 3.85 (s, 9H; OCH_3), 4.84 (d, J=13.7 Hz, 3H; CH_2), 6.96 (s, 3H; aryl C*H*), 7.09 (s, 3H; aryl C*H*), 7.71 (dd, J=1.5, 4.5 Hz, 6H; pyH3/H5), 8.47 (s, 3H; NC*H*py), 8.73 ppm (dd, J=1.5, 4.5 Hz, 6H; pyH2/H6); ^{13}C NMR (CDCl$_3$): δ=36.96, 56.66, 114.07, 122.61, 123.80, 132.14, 139.34, 139.74, 143.46, 150.89, 151.20, 159.82 ppm. No further characterisation was undertaken as this compound decomposes slowly in solution and the solid state.

Part B: Yield: 61%; m.p. 169–71 °C; ^{1}H NMR (CDCl$_3$): δ=3.30 (d, J=13.7 Hz, 3H; CH_2), 3.51 (s, 9H; OCH_3), 4.36 (s, 6H; NHCH_2py), 4.62 (d overlapping br s, 6H; CH_2, NH), 6.29 (s, 3H; aryl C*H*), 6.37 (s, 3H; aryl C*H*), 7.27 (d, J=6 Hz, 6H; pyH3/H5), 8.52 ppm (d, J=6.0 Hz, 6H; pyH2/H6); ^{1}H NMR (CD$_2$Cl$_2$): δ=3.27 (d, J=13.7 Hz, 3H; CH_2), 3.53 (s, 9H; OCH_3), 4.37 (s, 6H; NHCH_2py), 4.58 (d, J=13.7 Hz, 3H; CH_2), 4.62 (br s, 3H; NH), 6.30 (s, 3H; aryl C*H*), 6.40 (s, 3H; aryl C*H*), 7.26 (d, J=5.9 Hz, 6H; pyH3/H5), 8.49 ppm (d, J=5.9 Hz, 6H; pyH2/H6); ^{1}H NMR (CD$_3$CN): δ=3.23 (d, J=13.7 Hz, 3H; CH_2), 3.50 (s, 9H; OCH_3), 4.40 (d, J=6.3 Hz, 6H; NHCH_2py), 4.51 (d, J=13.6 Hz, 3H; CH_2), 4.89 (t, J=6.4 Hz, 3H; NH), 6.38 (s, 3H; aryl C*H*), 6.50 (s, 3H; aryl C*H*), 7.22 (d, J=5.3 Hz, 6H; pyH3/H5), 8.44 ppm (d, J=4.7 Hz, 6H; pyH2/H6); ^{1}H NMR ([D$_6$]acetone): δ=3.17 (d, J=13.5 Hz, 3H; CH_2), 3.41 (s, 9H; OCH_3), 4.36 (s, 6H; NHCH_2py), 4.51 (d, J=13.5 Hz, 3H; CH_2), 5.00 (br s, 3H; NH), 6.38 (s, 3H; aryl C*H*), 6.46 (s, 3H; aryl C*H*), 7.21 (d, J=5.6 Hz, 6H; pyH3/H5), 8.37 ppm (d, J=5.9 Hz, 6H; pyH2/H6); ^{13}C NMR (CDCl$_3$): δ=36.87, 47.48, 55.82, 111.44, 111.50, 122.19, 128.74, 132.68, 136.51, 145.90, 150.16, 150.32 ppm; ^{13}C NMR (CD$_2$Cl$_2$): δ=36.92, 47.64, 56.33, 111.69, 111.84, 122.51, 128.85, 133.03, 137.03, 146.36, 150.41, 150.69 ppm; HRMS (ES+): calcd for $C_{42}H_{43}N_6O_3^+$: 679.3397; found:

679.3386; elemental analysis calcd (%) for $C_{42}H_{42}N_6O_3{\cdot}H_2O$: C 72.85, H 6.35, N 12.14; found: C 72.85, H 6.30, N 11.65.

Complexes of 3

Synthesis of $[Ag_2(3)_2(CH_3CN)_2][Co(C_2B_9H_{11})_2]_2{\cdot}2CH_3CN$ (5): A solution of $Ag[Co(C_2B_9H_{11})_2]$ (6.4 mg, 14.8 μmol) dissolved in acetonitrile and **3** (10.3 mg, 15.2 μmol) dissolved in acetone were mixed together and the solvent allowed to evaporate slowly in the dark. This gave large yellow block-shaped crystals. Yield: 14.2 mg, 79%; ^{1}H NMR (CD_3CN): $\delta = 8.33$ (d, $J = 3.8$ Hz, 3H; pyH6), 8.18 (s, 3H; pyH2), 7.80 (d, $J = 7.9$ Hz, 3H; pyH4), 7.40 (dd, $J = 5.2$, 7.8 Hz, 3H; pyH5), 6.52 (s, 3H; aryl H), 6.48 (s, 3H; aryl H), 4.82 (brs, 3H; NH), 4.53 (m, 9H; CH_2NH, Ar-CH_2-Ar), 3.86 (brs, 4H; carbaborane CH), 3.51 (s, 9H; OCH_3), 3.29 ppm (d, ^2J-(H,H) = 13.6 Hz, 3H; Ar-CH_2-Ar); ^{1}H NMR ([D$_6$]acetone): $\delta = 8.22$ (d, $J = 4.5$ Hz, 3H; pyH6), 8.03 (s, 3H; pyH2), 7.80 (d, $J = 7.9$ Hz, 3H; pyH4), 7.31 (dd, $J = 5.1$, 7.7 Hz, 3H; pyH5), 6.52 (s, 3H; aryl H), 6.49 (s, 3H; aryl H), 4.63 (d, ^2J(H,H) = 17.3 Hz, 3H; CH_2NH), 4.45 (m, 6H; CH_2NH, Ar-CH_2-Ar), 3.83 (brs, 4H; carbaborane CH), 3.40 (s, 9H; OCH_3), 3.14 ppm (d, ^2J(H,H) = 13.6 Hz, 3H; Ar-CH_2-Ar); IR (solid state): $\tilde{\nu} = 3425$, 3278, 3039, 2924, 2550 (B–H), 2289 (C≡N), 2254 (C≡N), 1612, 1592, 1522, 1477, 1460, 1408, 1358, 1314, 1267, 1221, 1195, 1146, 1099, 1088, 1045, 1020, 983, 922, 875, 847, 786, 742, 705, 619, 558, 529 cm^{-1}; elemental analysis calcd (%) for $C_{100}H_{140}B_{36}N_{16}O_6Co_2Ag_2$: C 50.35, H 5.93, N 9.40; found: C 50.25, H 5.85, N 9.15.

Reaction in the presence of benzonitrile: A solution of $Ag[Co(C_2B_9H_{11})_2]$ (3.2 mg, 7.4 μmol) dissolved in acetone and **3** (5.1 mg, 7.5 μmol) dissolved in acetone were mixed together, benzonitrile was added (excess) and the solvent was allowed to evaporate slowly in the dark. This gave a yellow precipitate that was collected, washed with small quantities of methanol and diethyl ether and dried in air. Yield 4.1 mg, 47%; ^{1}H NMR ([D$_6$]acetone): $\delta = 8.25$ (d, $J = 4.8$ Hz, 6H; pyH6), 8.00 (s, 6H; pyH2), 7.88 (d, $J = 8.0$ Hz, 6H; pyH4), 7.62 (m, 3H; C_6H_5CN), 7.45 (dd, $J = 5.1$, 7.8 Hz, 8H; pyH5, C_6H_5CN), 6.53 (s, 6H; aryl H), 6.50 (s, 6H; aryl H), 4.51 (m, 18H; CH_2NH, Ar-CH_2-Ar), 3.84 (brs, 8H; carbaborane CH), 3.39 (s, 18H; OCH_3), 3.19 ppm (d, $J = 13.4$ Hz, 6H; Ar-CH_2-Ar); IR (solid state): $\tilde{\nu} = 3647$, 3427, 3031, 2934, 2861, 2542 (B–H), 2227 (Ar-C≡N), 1614, 1522, 1477, 1460, 1434, 1408, 1359, 1317, 1257, 1223, 1195, 1146, 1097, 1074, 1051, 1018, 981, 922, 874, 847, 791, 741, 706, 687, 647, 618, 548, 532 cm^{-1}; elemental analysis calcd (%) for $C_{99}H_{137}B_{36}N_{13}O_8Co_2Ag_2$: C 50.38, H 5.86, N 7.72; found: C 50.15, H 5.85, N 7.25.

Reaction in the presence of (S)-(+)-2-methylbutarynitrile: Compounds **3** (5.1 mg, 7.5 μmol) and $Ag[Co(C_2B_9H_{11})_2]$ (3.2 mg, 7.4 μmol) were dissolved in [D$_6$]acetone (1 mL). (*S*)-(+)-2-Methylbutarynitrile (8 μL, 7.6 μmol) was added to the yellow solution. ^{1}H NMR ([D$_6$]acetone): $\delta =$ 8.18 (d, $J = 5.1$ Hz, 3H; pyH6), 7.89 (s, 3H; pyH2), 7.82 (d, $J = 10.7$ Hz, 3H; pyH4), 7.36 (dd, $J = 5.1$, 7.7 Hz, 3H; pyH5), 6.50 (s, 3H; aryl H), 6.46 (s, 3H; aryl H), 4.61 (d, $J = 7.3$ Hz, 3H; CH_2NH), 4.45 (m, 6H; CH_2NH, Ar-CH_2-Ar), 3.80 (brs, 4H; carbaborane CH), 3.37 (s, 9H; OCH_3), 3.18 (d, $J = 13.5$ Hz, 3H; Ar-CH_2-Ar), 2.91 (brs, water), 2.60 (m, 1H; C*H*CN), 1.50 (m, 2H; CH_3CH_2), 1.18 (d, $J = 7.1$ Hz, 3H; CH_3CHCN), 0.94 ppm (t, $J = 7.4$ Hz 3H; CH_3CH_2).

Synthesis of $[Ag_2(3)_2(CH_3CN)_2](CB_{11}H_{12})_2$ (6): Silver carbollide (3.8 mg, 0.015 mmol) was dissolved in acetonitrile and added to a solution of **3** (10.2 mg, 0.015 mmol) in acetone. Slow evaporation gave colourless block-shaped crystals. Yield 6.8 mg, 49%; IR (solid state): $\tilde{\nu} = 3421$, 2933, 2528 (B–H), 2289 (C≡N), 2250 (C≡N), 1613, 1522, 1462, 1408, 1357, 1316, 1266, 1221, 1195, 1144, 1097, 1021, 989, 943, 874, 846, 788, 741, 706, 644, 618, 528 cm^{-1}; elemental analysis calcd (%) for $C_{86}H_{108}B_{22}N_{12}O_6Ag_2$: C 55.54, H 5.87, N 9.04; found: C 55.60, H 5.95, N 9.30.

Synthesis of $[Ag_2(3)_2(CH_3CN)_2](CF_3SO_3)_2{\cdot}4CH_3CN$ (7): Silver triflate (4.5 mg, 0.018 mmol) and **3** (10.5 mg, 0.015 mmol) were both dissolved in acetonitrile. Vapour diffusion of diethyl ether into this solution gave colourless block-shaped crystals. Yield: 2.6 mg, 18%; IR (solid state): $\tilde{\nu} =$ 3425, 3346, 2925, 2290 (C≡N), 2257 (C≡N), 1613, 1599, 1514, 1477, 1439, 1407, 1355, 1316, 1257, 1221, 1195, 1145, 1098, 1071, 1049, 1029, 989, 937, 877, 847, 795, 777, 752, 741, 707, 636, 619, 571, 517 cm^{-1}; elemental analysis calcd (%) for $C_{90}H_{90}N_{14}O_{12}F_6S_2Ag_2$: C 55.32, H 4.65, N 10.04; found: C 55.00, H 4.70, N 10.15.

Synthesis of $\{[Ag(3)(H_2O)](SbF_6)\}_n$ (9): A solution of silver hexafluoroantimonate (5.0 mg, 14.5 μmol) dissolved in acetonitrile and **3** (10.4 mg, 15.3 μmol) dissolved in acetone were mixed together and the reaction mixture allowed to evaporate slowly to dryness in the dark. This gave an oily film from which colourless crystalline plates that were suitable for X-ray crystallography formed. Yield: 7.8 mg, 51%; ^{1}H NMR ([D$_6$]acetone): $\delta = 8.27$ (d, $J = 4.9$ Hz, 3H; pyH6), 8.03 (s, 3H; pyH2), 7.89 (d, $J = 7.8$ Hz, 3H; pyH4), 7.43 (dd, $J = 5.1$, 7.8 Hz, 3H; pyH5), 6.52 (s, 3H; aryl H), 6.48 (s, 3H; aryl H), 4.61 (d, $^2J = 17.2$ Hz, 3H; CH_2NH), 4.46 (m, 6H; CH_2NH, Ar-CH_2-Ar), 3.38 (s, 9H; OCH_3), 3.18 ppm (d, $^2J = 13.6$ Hz, 3H; Ar-CH_2-Ar); IR (solid state): $\tilde{\nu} = 3412$, 2979, 2938, 2837, 1615, 1520, 1463, 1409, 1361, 1317, 1257, 1222, 1200, 1148, 1097, 1076, 1049, 1025, 993, 947, 930, 880, 864, 849, 806, 792, 750, 706, 654, 618, 528, 508, 466 cm^{-1}; elemental analysis calcd (%) for $C_{42}H_{46}N_6O_5F_6AgSb$: C 47.66, H 4.39, N 7.94; found: C 47.25, H 4.15, N 7.65.

Synthesis of complexes of 4

Synthesis of $[Ag_4(4)_4(CH_3CN)_3]\cap(CH_3CN)_4(PF_6)_4{\cdot}9.5CH_3CN{\cdot}0.5H_2O$ (10): A solution of silver hexafluorophosphate (5.9 mg, 0.023 mmol) dissolved in acetonitrile (1 mL) and **4** (14.5 mg, 0.021 mmol) dissolved in acetonitrile (2 mL) were mixed together and concentrated by slow evaporation in the dark. Slow vapour diffusion of diethyl ether into this solution gave colourless crystals suitable for X-ray diffraction studies. Yield: 10.1 mg, 52%; ^{1}H NMR (CD_3CN, 233 K): $\delta = 8.47$ (d, $J = 5.4$ Hz, 6H; pyH2/H6), 6.73 (d, $J = 5.4$ Hz, 3H; pyH3/H5), 6.21 (s, 3H; aryl H), 6.18 (s, 3H; aryl H), 4.65 (m, 3H; CH_2NH), 4.29 (m, 6H; Ar-CH_2-Ar, CH_2NH), 3.52 (t, $J = 7.1$ Hz, 3H; NH), 3.12 (d, $J = 13.5$ Hz, 3H; Ar-CH_2-Ar), 2.88 (s, 9H; OCH_3); ^{1}H NMR (CD_3CN, 333 K): $\delta = 8.46$ (d, $J =$ 4.6 Hz, 6H; pyH2/H6), 7.32 (d, $J = 4.6$ Hz, 3H; pyH3/H5), 6.74 (s, 3H; aryl H), 6.46 (s, 3H; aryl H), 4.59 (d, $J = 13.6$ Hz, 3H; Ar-CH_2-Ar), 4.45 (q, $J = 17.0$ Hz, 6H; CH_2NH), 3.61 (s, 9H; OCH_3), 3.30 ppm (d, $J =$ 13.7 Hz, 3H; Ar-CH_2-Ar); IR (solid state): $\tilde{\nu} = 3635$, 3429, 2934, 1710, 1607, 1560, 1516, 1461, 1423, 1360, 1312, 1266, 1222, 1198, 1147, 1066, 1017, 984, 939, 925, 877, 839, 794, 741, 618, 557, 477 cm^{-1}; MALDI MS: *m*/*z* (%): 1718.2 (4) $[Ag_4(\mathbf{4})_4(PF_6)_2]^{2+}$, 785.3 (100) $[Ag(\mathbf{4})]^+$, 678.4 (55) $[\mathbf{4}{+}H]^+$; elemental analysis calcd (%) for $C_{168}H_{168}N_{24}O_{12}F_{24}P_4Ag_4$ C 54.14, H 4.55, N 9.02; found: C 52.55, H 4.65, N 9.55%.

Synthesis of $[Ag_4(4)_4(CH_3CN)_3]\cap(CH_3CN)_4(SbF_6)_4{\cdot}5CH_3CN$ (11): A solution of silver hexafluoroantimonate (6.0 mg, 0.017 mmol) dissolved in acetonitrile (1.5 mL) and **4** (11.2 mg, 0.016 mmol) dissolved in 2,2,2-trifluoroethanol (1.5 mL) were mixed together and concentrated by slow evaporation in the dark. Slow vapour diffusion of diethyl ether into this solution gave very small colourless crystals which rapidly lose solvent on removal from the mother liquor. Yield: 3.5 mg, 22%; ^{1}H NMR (CD_3CN): $\delta = 8.46$ (d, $J = 6.0$ Hz, 6H; pyH2/H6), 6.99 (brs, 6H; pyH3/H5), 6.25 (brs, 3H; aryl H), 6.18 (brs, 3H; aryl H), 4.55 (d, $J = 18.9$ Hz, 3H; CH_2NH), 4.40 (d, $J = 13.6$ Hz, 3H; Ar-CH_2-Ar), 4.30 (d, $J = 18.9$ Hz, 3H; CH_2NH), 3.13 ppm (brm, 12H; OCH_3, Ar-CH_2-Ar); IR (solid state): $\tilde{\nu} =$ 3635, 3431, 2935, 1607, 1560, 1516, 1458, 1423, 1360, 1312, 1264, 1221, 1198, 1146, 1066, 1017, 984, 939, 924, 850, 796, 742, 656, 618, 477 cm^{-1}; elemental analysis calcd (%) for $C_{168}H_{168}N_{24}O_{12}F_{24}Sb_4Ag_4$: C 49.34, H 4.15, N 8.22; found: C 48.50, H 4.20, N 7.85.

Synthesis of $\{[Ag(4)\{N{\equiv}C(CH_2)_3C{\equiv}N\}]PF_6\cap(N{\equiv}C(CH_2)_3C{\equiv}N)\}_n$ (12): A solution of silver hexafluorophosphate (3.8 mg, 0.015 mmol) dissolved in acetonitrile (1 mL) and **4** (10.0 mg, 0.015 mmol) dissolved in acetonitrile (2 mL) were mixed together. Ten drops of glutaronitrile (excess) were added and the resulting solution concentrated by slow evaporation in the dark to yield very pale brown/colourless crystals amongst a brown sludge. These were washed with acetone and ethanol and dried in vacuo. Yield: 5.3 mg, 32%; IR (solid state): $\tilde{\nu} = 3433$, 2920, 2249 (C≡N stretch), 1608, 1561, 1520, 1462, 1423, 1362, 1312, 1267, 1229, 1198, 1149, 1067, 1011, 985, 939, 925, 833, 800, 742, 619, 557, 478 cm^{-1}. Suitable combustion analysis could not be obtained for this compound as the crystals were very difficult to isolate.

Synthesis of $\{[Ag(4)\{N{\equiv}C(CH_2)_3C{\equiv}N\}]\cap(N{\equiv}C(CH_2)_3C{\equiv}N)[Co(C_2B_9H_{11})_2]{\cdot}(N{\equiv}C(CH_2)_3C{\equiv}N)\}_n$ (13): A solution of silver cobalticarbaborane (3.5 mg, 8.1×10^{-3} mmol) dissolved in acetonitrile (2 mL) and **4** (5.3 mg, 7.8×10^{-3} mmol) dissolved in 2,2,2-trifluoroethanol (2 mL) were mixed together. An excess of glutaronitrile was added and the resulting

solution concentrated by slow evaporation in the dark to yield yellow crystals with a needle morphology. Yield: 4.5 mg, 41%; IR (solid state): $\tilde{\nu}$ = 3427, 2936, 2551 (B–H), 2252 (C≡N), 2200 (C≡N), 1608, 1562, 1518, 1459, 1421, 1406, 1362, 1312, 1271, 1250, 1222, 1198, 1146, 1091, 1072, 1062, 1022, 982, 939, 924, 875, 851, 800, 740, 721, 618, 589, 474 cm^{-1}; elemental analysis calcd (%) for $C_{56}H_{76}N_{10}O_3B_{18}CoAg$: C 51.78, H 5.91, N 10.79; found: C 51.00, H 5.80, N 11.00.

X-ray crystallography: In general, crystals were mounted under oil or grease onto a glass fibre and X-ray data collected at low temperatures with $Mo_{K\alpha}$ radiation (λ = 0.71073 Å). At the University of Leeds data was collected either on a Nonius KappaCCD diffractometer or on a Bruker Nonius FR591 diffractometer, fitted with an ApexII detector.[45] The rotating anode was operated at 4 kW for data collections reported herein. Three data sets (compounds **4**, **11** and **13**) were collected at CCLRC Daresbury Laboratory, Station 16.2SMX, on a Bruker Nonius ApexII detector[46] with synchotron radiation with a wavelength of λ = 0.84640 Å. Data were corrected for polarisation and Lorenztian effects, and absorption corrections applied using a multiscan method (SORTAV/SADABS).[47] Structures were solved by direct methods by using SHELXS-97[48] and refined by full-matrix least-squares on F^2 by SHELXL-97.[49] Unless otherwise stated, all non-hydrogen atoms were refined anisotropically and hydrogen atoms were included as invariants at geometrically estimated positions. Diagrams were generated using the program X-Seed[50] as an interface to POV-Ray. Additional refinement details for individual structures are described below. CCDC-292530–292539 contain the supplementary crystallographic data for this paper. These data can be obtained free of charge from The Cambridge Crystallographic Data Centre via www.ccdc.cam.ac.uk/data_request/cif.

Crystal data for $(\mathbf{2})_2{\cdot}CH_3COCH_3$: $C_{87}H_{90}N_{12}O_7$, M_r = 1415.71, triclinic, $P\bar{1}$, a = 13.4947(2), b = 14.7438(3), c = 21.1834(4) Å, α = 73.2290(8), β = 85.4170(8), γ = 70.0233(9)°, V = 3791.82(12) Å^3, Z = 2, ρ_{calcd} = 1.240 Mg cm^{-3}, μ = 0.080 mm^{-1}, $F(000)$ = 1504, colourless plate, 0.38 × 0.15 × 0.02 mm, $2\theta_{max}$ = 48.22°, T = 150(1) K, 52037 reflections, 12029 unique (99.7% completeness), R_{int} = 0.0739, 963 parameters, GOF = 1.009, $wR2$ = 0.1538 for all data, R_1 = 0.0519 for 8680 data with $I > 2\sigma(I)$.

Crystal data for $\mathbf{4}{\cdot}CH_3OH$: $C_{43}H_{46}N_6O_4$, M_r = 710.86, orthorhombic, *Pbca*, a = 13.8900(12), b = 10.4606(9), c = 51.319(5) Å, V = 7456.5(11) Å^3, Z = 8, ρ_{calcd} = 1.266 Mg cm^{-3}, μ = 0.083 mm^{-1}, $F(000)$ = 3024, colourless block, 0.14 × 0.09 × 0.04 mm, $2\theta_{max}$ = 59.22°, T = 150(1) K, 41562 reflections, 6169 unique (99.0% completeness), R_{int} = 0.0812, 483 parameters, GOF = 1.042, $wR2$ = 0.1409 for all data, R_1 = 0.0522 for 4734 data with $I > 2\sigma(I)$.

Crystal data for $[Ag_2(\mathbf{3})_2(CH_3CN)_2][Co(C_2B_9H_{11})_2]_2{\cdot}2\,CH_3CN$ (**5**): $C_{100}H_{140}Ag_2B_{36}Co_2N_{16}O_6$, M_r = 2385.04, monoclinic, $P2_1/n$, a = 20.0373(3), b = 12.1108(2), c = 24.3168(4) Å, β = 95.0293(9)°, V = 5878.18(16) Å^3, Z = 2, ρ_{calcd} = 1.348 Mg cm^{-3}, μ = 0.664 mm^{-1}, $F(000)$ = 2456, yellow prism, 0.34 × 0.14 × 0.12 mm, $2\theta_{max}$ = 50.06°, T = 150(1) K, 44031 reflections, 10350 unique (99.6% completeness), R_{int} = 0.0542, 735 parameters, GOF = 1.046, $wR2$ = 0.1292 for all data, R_1 = 0.0447 for 8296 data with $I > 2\sigma(I)$.

Crystal data for $\{[Ag(\mathbf{3})(H_2O)](SbF_6)\}_n$ (**9**): $C_{42}H_{44}AgF_6N_6O_4Sb$, M_r = 1040.45, monoclinic, $C2/c$, a = 35.7790(8), b = 15.0388(4), c = 17.8896(6) Å, β = 117.4508(11)°, V = 8542.1(4) Å^3, Z = 8, ρ_{calcd} = 1.618 Mg cm^{-3}, μ = 1.166 mm^{-1}, $F(000)$ = 4176, colourless plate, 0.26 × 0.12 × 0.02 mm, $2\theta_{max}$ = 53.46°, T = 150(1) K, 33767 reflections, 9036 unique (99.5% completeness), R_{int} = 0.0790, 544 parameters, GOF = 1.027, $wR2$ = 0.1218 for all data, R_1 = 0.0485 for 6208 data with $I > 2\sigma(I)$. Additional crystallographic information: The hydrogen atoms on the coordinated water molecule could not be located in the Fourier difference map.

Crystal data for $[Ag_4(\mathbf{4})_4(CH_3CN)_3]\cap(CH_3CN)_4(SbF_6)_4{\cdot}5\,CH_3CN$ (**11**): $C_{192}H_{204}Ag_4F_{24}N_{36}O_{12}Sb_4$, M_r = 4582.39, monoclinic, $P2_1/c$, a = 23.5333(12), b = 28.9784(15), c = 36.4796(19) Å, β = 126.534(1)°, V = 19989.2(18) Å^3, Z = 4, ρ_{calcd} = 1.523 Mg cm^{-3}, μ = 1.004 mm^{-1}, $F(000)$ = 9248, colourless triangular plate, 0.13 × 0.08 × 0.02 mm, $2\theta_{max}$ = 54.00°, T = 150(1) K, 104506 reflections, 25785 unique (99.7% completeness), R_{int} = 0.1128, 2457 parameters, GOF = 1.038, $wR2$ = 0.1909 for all data, R_1 = 0.0680 for 16941 data with $I > 2\sigma(I)$. Additional crystallographic information: The tetramer structure is very similar to the BF_4^- analogue previously reported. The structure was refined using only data to a theta angle of 27°. The carbon atoms of a coordinated acetonitrile molecule were refined with anisotropic displacement parameters as was the methyl group of a solvate acetonitrile molecule. Restraints were used to maintain chemically sensible bond lengths for a guest acetonitrile molecule (by the SAME command) and for a coordinated acetonitrile molecule.

Crystal data for $\{[Ag(\mathbf{4})\{N{\equiv}C(CH_2)_3C{\equiv}N\}]\cap(N{\equiv}C(CH_2)_3C{\equiv}N)[Co(C_2B_9H_{11})_2]{\cdot}(N{\equiv}C(CH_2)_3C{\equiv}N)\}_n$ (**13**): $C_{61}H_{82}AgB_{18}CoN_{12}O_3$, M_r = 1392.77, monoclinic, $C2/c$, a = 33.1714(17), b = 21.5803(11), c = 21.4586(11) Å, β = 113.443(1)°, V = 14093.1(12) Å^3, Z = 8, ρ_{calcd} = 1.313 Mg cm^{-3}, μ = 0.566 mm^{-1}, $F(000)$ = 5760, yellow rod, 0.25 × 0.08 × 0.03 mm, $2\theta_{max}$ = 50.98°, T = 150(1) K, 46930 reflections, 12966 unique (99.0% completeness), R_{int} = 0.0621, 843 parameters, GOF = 1.056, $wR2$ = 0.2594 for all data, R_1 = 0.0834 for 8834 data with $I > 2\sigma(I)$. Additional crystallographic information: The silver atom was modelled over two positions. The cobalticarbaborane anion in the structure had large anisotropic displacement parameters associated with dynamic disorder of the carbon and boron positions. The channel bound glutaronitrile molecule was refined with isotropic displacement parameters and restrained to have bond lengths similar to the guest glutaronitrile with the SAME command. The coordinated glutaronitrile ligand was similarly treated with restraints on the bond lengths. Two peaks in the Fourier difference map (1.80 and 1.64 eÅ^3) and located within the channels of the structure were not modelled.

Acknowledgements

We thank the EPSRC for financial support and the EPSRC National Mass Spectrometry Service Centre in Swansea for provision of mass spectrometry on the $[Ag_4(\mathbf{4})_4]$ complexes. Prof. Gareth Morris is thanked for provision of the script that enabled phase and baseline correction of spectra prior to generation of the DOSY plots. Additionally, we would like to thank Mr. Simon Barrett for variable temperature NMR measurements and Mr. Martin Huscroft for microanalysis.

[1] J. W. Steed, H. Zhang, J. L. Atwood, *Supramol. Chem.* **1996**, *7*, 37–45.

[2] a) B. T. Ibragimov, K. K. Makhkamov, K. M. Beketov, *J. Inclusion Phenom. Macrocyclic Chem.* **1999**, *35*, 583–593; b) M. J. Hardie, P. D. Godfrey, C. L. Raston, *Chem. Eur. J.* **1999**, *5*, 1828–1833; J. L. Atwood, M. J. Barnes, M. G. Gardiner, C. L. Raston, *Chem. Commun.* **1996**, 1449–1450; c) J. W. Steed, P. C. Junk, J. L. Atwood, M. J. Barnes, C. L. Raston, R. S. Burkhalter, *J. Am. Chem. Soc.* **1994**, *116*, 10346–10347; d) D. V. Konarev, S. S. Khasanov, I. I. Vorontsov, G. Saito, M. Y. Antipin, A. Otsuka, R. N. Lyubovskaya, *Chem. Commun.* **2002**, 2548–2549; e) K. T. Holman, J. W. Steed, J. L. Atwood, *Angew. Chem.* **1997**, *109*, 1840–1842; *Angew. Chem. Int. Ed. Engl.* **1997**, *36*, 1736–1738; f) M. J. Hardie, C. L. Raston, *Chem. Commun.* **2001**, 905–906.

[3] For reviews and examples, see: a) A. Collet, J. P. Dutasta, B. Lozach, J. Canceill, *Top. Curr. Chem.* **1993**, *165*, 103–129; b) A. Collet, *Tetrahedron* **1987**, *43*, 5725–5759; c) T. Brotin, J.-P. Dutasta, *Eur. J. Org. Chem.* **2003**, 973–984; d) T. Brotin, V. Roy, J.-P. Dutasta, *J. Org. Chem.* **2005**, *70*, 6187–6195; e) T. Brotin, T. Devic, A. Lesage, L. Emsley, A. Collet, *Chem. Eur. J.* **2001**, *7*, 1561–1573; f) M. Darzac, T. Brotin, L. Rousset-Arzel, D. Bouchu, J.-P. Dutasta, *New J. Chem.* **2004**, *28*, 502–512; g) A. Gautier, J.-C. Mulatier, J. Crassous, J.-P. Dutasta, *Org. Lett.* **2005**, *7*, 1207–1210; h) S. T. Mough, J. C. Goeltz, K. T. Holman, *Angew. Chem.* **2004**, *116*, 5749–5753; *Angew. Chem. Int. Ed.* **2004**, *43*, 5631–5635.

[4] a) R. Ahmad, M. J. Hardie, *CrystEngComm* **2002**, *4*, 227–231; b) M. J. Hardie, *Struct. Bonding* **2004**, *111*, 139–174.

[5] M. J. Hardie, R. Ahmad, C. J. Sumby, *New J. Chem.* **2005**, *29*, 1231–1240.

[6] G. P. F. van Strijdonck, J. A. E. H. van Haare, J. G. M. van der Linden, J. J. Steggerda, R. J. M. Nolte, *Inorg. Chem.* **1994**, *33*, 999–1000.

[7] G. Veriot, J.-P. Dutasta, G. Matouzenko, A. Collet, *Tetrahedron* **1995**, *51*, 389–400.
[8] a) J. A. Wytko, J. Weiss, *J. Inclusion Phenom. Mol. Recognit. Chem.* **1994**, *19*, 207–225; b) J. A. Wytko, C. Boudon, J. Weiss, M. Gross, *Inorg. Chem.* **1996**, *35*, 4469–4477; c) J. A. Wytko, J. Weiss, *Tetrahedron Lett.* **1991**, *32*, 7261–7264.
[9] Z. Zhong, A. Ikeda, S. Shinkai, S. Sakamoto, K. Yamaguchi, *Org. Lett.* **2001**, *3*, 1085–1087.
[10] M. J. Hardie, R. M. Mills, C. J. Sumby, *Org. Biomol. Chem.* **2004**, *2*, 2958–2964.
[11] a) M. J. Hardie, C. J. Sumby, *Inorg. Chem.* **2004**, *43*, 6872–6874; b) C. J. Sumby, M. J. Hardie, *Cryst. Growth Des.* **2005**, *5*, 1321–1324.
[12] For reviews, see: a) S. Leininger, B. Olenyuk, P. J. Stang, *Chem. Rev.* **2000**, *100*, 853–908; b) B. J. Holliday, C. A. Mirken, *Angew. Chem.* **2001**, *113*, 2076–2097; *Angew. Chem. Int. Ed.* **2001**, *40*, 2022–2043; c) T. D. Hamilton, L. R. MacGillivray, *Cryst. Growth Des.* **2004**, *4*, 419–430; d) P. J. Steel, *Acc. Chem. Res.* **2005**, *38*, 243–250.
[13] For example, see: M. Fujita, S. Nagao, K. Ogura, *J. Am. Chem. Soc.* **1995**, *117*, 1649–1650.
[14] For example, see: M. Tominaga, K. Suzuki, M. Kawano, T. Kusukawa, T. Ozeki, S. Sakamoto, K. Yamaguchi, M. Fujita, *Angew. Chem.* **2004**, *116*, 5739–5743; *Angew. Chem. Int. Ed.* **2004**, *43*, 5621–5625.
[15] For examples, see: a) K. Kobayashi, Y. Yamada, M. Yamanaka, Y. Sei, K. Yamaguchi, *J. Am. Chem. Soc.* **2004**, *126*, 13896–13897; b) R. Pinalli, V. Cristini, V. Sottili, S. Geremia, M. Campagnolo, A. Caneschi, E. Dalcanale, *J. Am. Chem. Soc.* **2004**, *126*, 6516–6517; c) B. Bibal, B. Tinant, J.-P. Declercq, J. P. Dutasta, *Chem. Commun.* **2002**, 432–433; d) S. J. Park, J.-I. Hong, *Chem. Commun.* **2001**, 1554–1555; e) M. J. Hardie, C. L. Raston, *J. Chem. Soc. Dalton Trans.* **2000**, 2483–2492; f) L. R. MacGillivray, P. R. Diamente, J. L. Reid, J. A. Ripmeester, *Chem. Commun.* **2000**, 359–360; g) J. Rebek, *Chem. Commun.* **2000**, 637–643; h) O. D. Fox, N. K. Dalley, R. G. Harrison, *Inorg. Chem.* **2000**, *39*, 620–622; i) P. Jacopozzi, E. Dalcanale, *Angew. Chem.* **1997**, *109*, 665–667; *Angew. Chem. Int. Ed. Engl.* **1997**, *36*, 613–615.
[16] O. D. Fox, M. G. B. Drew, P. D. Beer, *Angew. Chem.* **2000**, *112*, 139–144; *Angew. Chem. Int. Ed.* **2000**, *39*, 135–140.
[17] O. D. Fox, E. J. S. Wilkinson, P. D. Beer, M. G. B. Drew, *Chem. Commun.* **2000**, 391–392.
[18] R. M. McKinlay, P. K. Thallapally, G. W. V. Cave, J. L. Atwood, *Angew. Chem.* **2005**, *117*, 5879–5882; *Angew. Chem. Int. Ed.* **2005**, *44*, 5733–5736.
[19] a) L. R. MacGillivray, J. L. Atwood, *Nature* **1997**, *389*, 469–472; b) G. W. V. Cave, J. Antesberger, L. J. Barbour, R. M. McKinlay, J. L. Atwood, *Angew. Chem.* **2004**, *116*, 5375–5378; *Angew. Chem. Int. Ed.* **2004**, *43*, 5263–5266.
[20] C. J. Sumby, M. J. Hardie, *Angew. Chem.* **2005**, *117*, 6553–6557; *Angew. Chem. Int. Ed.* **2005**, *44*, 6395–6399.
[21] C. Garcia, J. Malthete, A. Collet, *Bull. Soc. Chim. Fr.* **1993**, *130*, 93–95.
[22] D. S. Bohle, D. J. Stasko, *Inorg. Chem.* **2000**, *39*, 5768–5770.
[23] M. J. Hardie, C. J. Sumby, unpublished results.
[24] a) A. Collet, J. Gabard, J. Jacques, M. Cesario, J. Guilhem, C. Pascard, *J. Chem. Soc. Perkin Trans. 1* **1981**, 1630–1638; b) Q.-P. Hu, M.-L. Ma, X.-F. Zheng, J. Reiner, L. Su, *Acta Crystallogr. Sect. E* **2004**, *60*, o1178–o1179.
[25] a) R. Ahmad, M. J. Hardie, *Supramol. Chem.* **2006**, *18*, 29–38; b) S. Q. Wang, G. Zeng, X. F. Zheng, K. Zhao, *Acta Crystallogr. Sect. E* **2003**, *59*, o1862–o1863; c) J. L. Scott, D. R. MacFarlane, C. L. Raston, C. M. Teoh, *Green Chem.* **2000**, *2*, 123–126.
[26] V. V. Krishnan, *J. Magn. Reson.* **1997**, *124*, 468–473.
[27] a) K. S. Cameron, L. Fielding, *J. Org. Chem.* **2001**, *66*, 6891–6895; b) F. W. Kotch, V. Sidorov, Y.-F. Lam, K. J. Kayser, H. Li, M. S. Kaucher, J. T. Davis, *J. Am. Chem. Soc.* **2003**, *125*, 15140–15150; c) T. Haino, Y. Matsumoto, Y. Fukazawa, *J. Am. Chem. Soc.* **2005**, *127*, 8936–8937.
[28] T. Haino, M. Kobayashi, M. Chikaraishi, Y. Fukazawa, *Chem. Commun.* **2005**, 2321–2323.
[29] M. S. Kaucher, Y.-F. Lam, S. Pieraccini, G. Gottarelli, J. T. Davis, *Chem. Eur. J.* **2005**, *11*, 164–173.
[30] The "molecular volume" command of the crystallography program X-Seed was used to provide a volume for the various components under study from which a radius could be calculated. This is not an entirely rigorous approach as none of the compounds under consideration is strictly spherical, but nonetheless provides several useful numbers as comparison to the theoretical literature values quoted in the text. The poorest approximation is for the cavitands **2** and **4**, which are bowl shaped with undefined solution conformations. Better approximations were obtained for the ellipsoid-shaped $[Ag_2(\mathbf{3})_2]$ capsule and almost spherical $[Ag_4(\mathbf{4})_4]$ prism.
[31] C. G. Claessens, T. Torres, *J. Am. Chem. Soc.* **2002**, *124*, 14522–14523.
[32] A. Ikeda, H. Udzu, Z. Zhong, S. Shinkai, S. Sakamoto, K. Yamaguchi, *J. Am. Chem. Soc.* **2001**, *123*, 3872–3877.
[33] W.-Y. Sun, J. Fan, T.-A. Okamura, J. Xie, K.-B. Yu, N. Ueyama, *Chem. Eur. J.* **2001**, *7*, 2557–2562.
[34] Additional details of the π-stacking interactions in structure **9**: centroid–centroid distances 3.958 Å; closest separation between atoms in plane 3.519 Å; slip angles of 18.14° and horizontal displacement of the centroids of 1.409 Å.
[35] C. Janiak, *J. Chem. Soc. Dalton Trans.* **2000**, 3885–3896.
[36] For example, see: a) E. Lozano, M. Nieuwenhuyzen, S. L. James, *Chem. Eur. J.* **2001**, *7*, 2644–2651; b) M.-C. Brandys, R. J. Puddephatt, *J. Am. Chem. Soc.* **2001**, *123*, 4839–4840; c) M.-C. Brandys, R. J. Puddephatt, *Chem. Commun.* **2001**, 1508–1509; d) T. J. Burchell, D. J. Eisler, M. C. Jennings, R. J. Puddephatt, *Chem. Commun.* **2003**, 2228–2229; e) P. Miller, M. Nieuwenhuyzen, J. P. H. Charmant, S. L. James, *CrystEngComm* **2004**, *6*, 408–412; f) N. L. S. Yue, M. C. Jennings, R. J. Puddephatt, *Chem. Commun.* **2005**, 4792–4794; g) T. J. Burchell, R. J. Puddephatt, *Inorg. Chem.* **2005**, *44*, 3718–3730.
[37] a) P. J. Steel, C. J. Sumby, *Inorg. Chem. Commun.* **2002**, *5*, 323–327; b) D. L. Reger, R. P. Watson, J. R. Gardinier, M. D. Smith, *Inorg. Chem.* **2004**, *43*, 6609–6619; c) R. Ahmad, M. J. Hardie, *New J. Chem.* **2004**, *28*, 1315–1319.
[38] A. J. Amoroso, J. C. Jeffery, P. L. Jones, J. A. McCleverty, P. Thornton, M. D. Ward, *Angew. Chem.* **1995**, *107*, 1577–1580; *Angew. Chem. Int. Ed. Engl.* **1995**, *34*, 1443–1445.
[39] a) D. L. Caulder, K. N. Raymond, *Acc. Chem. Res.* **1999**, *32*, 975–982; b) D. L. Caulder, C. Bruckner, R. E. Powers, S. Konig, T. N. Parac, J. A. Leary, K. N. Raymond, *J. Am. Chem. Soc.* **2001**, *123*, 8923–8938.
[40] M. Albrecht, I. Janser, S. Meyer, P. Weis, R. Frohlich, *Chem. Commun.* **2003**, 2854–2855.
[41] D. Fiedler, D. H. Leung, R. G. Bergman, K. N. Raymond, *Acc. Chem. Res.* **2005**, *38*, 349–358.
[42] S. P. Argent, T. Riis-Johannessen, J. C. Jeffery, L. P. Harding, M. D. Ward, *Chem. Commun.* **2005**, 4647–4649.
[43] R. M. Yeh, J. Xu, G. Seeber, K. N. Raymond, *Inorg. Chem.* **2005**, *44*, 6228–6239.
[44] M. D. Pelta, H. Barjat, G. A. Morris, A. L. Davis, S. J. Hammond, *Magn. Reson. Chem.* **1998**, *36*, 706–714.
[45] M. D. Pelta, G. A. Morris, M. J. Stchedroff, S. J. Hammond, *Magn. Reson. Chem.* **2002**, *40*, S147-S152.
[46] Bruker, APEXII, Bruker AXS inc. Madison, Wisconsin, USA, **2004**.
[47] a) R. H. Blessing, *Acta Crystallogr. Sect. A* **1995**, *51*, 33–38; b) R. H. Blessing, *J. Appl. Crystallogr.* **1997**, *30*, 421–426.
[48] G. M. Sheldrick, *Acta Crystallogr. Sect. A* **1990**, *46*, 467–473.
[49] G. M. Sheldrick, SHELXL-97, University of Göttingen, Germany, **1997**.
[50] L. J. Barbour, J. L. Atwood, *Cryst. Growth Des.* **2003**, *3*, 3–8.

Received: December 9, 2005
Published online: February 21, 2006

